UNIVERSITY OF ILLINOIS ENGINEERING EXPERIMENT STATION
Bulletin Series No. 408

STRESS DISTRIBUTION AND STRENGTH CONDITION OF TWO ROLLING CYLINDERS PRESSED TOGETHER

EUGENE I. RADZIMOVSKY
Research Associate in Mechanical Engineering

Published by the University of Illinois, Urbana

3500—11-52—50311

UNIVERSITY
OF ILLINOIS
:: PRESS ::

CONTENTS

I. INTRODUCTION 5
1. Purpose and Scope of Investigation 5
2. Acknowledgments 6
II. PREVIOUS DATA ON CHARACTER OF FAILURE OF VARIOUS MACHINE MEMBERS 8
3. Character of Fatigue Failure of Gear Teeth and Ball and Roller Bearings 8
4. Experimental Investigations with Roller Machines 8
III. DISTRIBUTION OF STRESSES IN ZONE OF CONTACT 10
5. H. Hertz' Investigation 10
6. Later Investigations of the Hertz Problem 12
7. Factors of the Hertz Problem Not Considered 14
8. Strength Calculation of Materials Based on Data Obtained from Stress Distribution Along the Plane of Symmetry 15
IV. ANALYSIS OF STRESS VARIATION IN CONTACT ZONE OF TWO COMPRESSED CYLINDERS ROLLING TOGETHER 17
9. Method of Influence Lines of Stresses 17
10. Analytical Method of Analysis 20
11. Stress Variation in Contact Zone Caused by Rolling 21
V. STRENGTH CONDITIONS OF MATERIALS SUBJECTED TO VARIABLE CONTACT STRESSES 26
12. Huber-Mises' Condition on Static Loading 26
13. General Case of Plane Stress Condition Due to Variable Loading 27
14. Endurance Limit of Steels Subjected to Variable Compressive Stress 27
15. Strength Condition of Materials Subjected to Contact Stresses Produced by Two Cylinders Rolling 29
VI. RESULTS OF INVESTIGATIONS USING THE SUGGESTED STRENGTH CONDITION 32
VII. SUMMARY AND CONCLUSIONS 35
APPENDIX A. TRANSFORMATION OF EQ. 17 IN TERMS OF THE STRESS COMPONENTS 37
APPENDIX B. TRANSFORMATION OF EQ. 19 IN TERMS OF THE STRESS COMPONENTS 39
APPENDIX C. REDUCTION OF VARIABLE STRESSES TO STATICAL CONDITIONS 40

FIGURES

1. Pressure Distribution on Contact Surface 11
2. Pressure Distribution Across the Strip of Contact Surface of Two Cylinders 12
3. Distribution of Stresses in Contact Zone Along Line of Symmetry 13
4. Pressure Distribution With and Without Lubricant, According to Eichinger 15
5. Variation in Value of Reduced Stress Along Axis of Symmetry, According to Eichinger 16
6. Single Concentrated Force Acting Perpendicular to a Plane 18
7. Influence Lines of Stresses Due to a Single Concentrated Force 18
8. Method Using Influence Lines of Stresses, Caused by a Series of Concentrated Forces 19
9. Variation of Stress Components in Contact Zone During Loading Cycle 23
10. Variation of Normal Stresses on Contact Surface During Loading Cycle 24
11. Strength Limits of Steels Subjected to Asymmetrical Loading Cycles 29
12. Surface Endurance Limit of Two Rolling Cylinders 33
13. Comparison Between Data from Eq. 28 and Experimental Results 34
14. Goodman's Linear Strength Relationship 40

TABLES

1. Maximum Values of Stress in Contact Zone in Terms of p_{max} 25
2. Mechanical Properties of Steels 32
3. Coefficients *A*, *B*, and *C*, and the Ratio, *K*, Between Critical Pressure on the Surface and Yield Point of Different Steels, for Various Layers Below Contact Surface 32

UNIVERSITY OF ILLINOIS ENGINEERING EXPERIMENT STATION

Bulletin Series No. 407

HEAT SUPPLIED TO I=B=R RESEARCH HOME FROM THE INSIDE CHIMNEY

WARREN S. HARRIS

Research Professor of Mechanical Engineering

ROSS J. MARTIN

Associate Professor of Mechanical Engineering

Published by the University of Illinois, Urbana

4500—1-53—49770

UNIVERSITY
OF ILLINOIS
:: PRESS ::

ABSTRACT

This bulletin presents a discussion of the useful heat supplied to the I = B = R Research Home from the inside chimney when the house was being heated by an oil-fired, forced-circulation, hot-water heating system. The data on which this discussion is based were obtained largely during the winters of 1941-42 and 1942-43.

The tests included in this discussion were made while operating the heating system with the flow control valve locked open so that gravity circulation of water occurred when the circulator was not in operation. The burner and circulator operation was controlled by the room thermostat alone, with no provision made for heating domestic hot water. An oil burning rate of 1.1 gal per hr was used. This rate was the minimum obtainable with a clean fire and with a CO_2 content of the flue gases not less than 8 percent at the smoke outlet of the boiler. The oil used weighed 7 lb per gal and had a calorific value of 19,550 Btu per lb. In order to keep a constant draft on the boiler at all times, a draft regulator was installed in the flue pipe connecting the boiler to the chimney.

Two methods of computing the heat supplied to the house from the chimney were used. The first method was based on observed flue gas temperatures and rates of flow; the second was based on observed temperatures of the plaster wall surrounding the chimney and of the room air. The nature of the heat flow from the chimney to the house did not lend itself to exact measurement. However, a comparison of the results obtained by the two independent methods indicated that, for the use made of them in this bulletin, the accuracy of the results by either method was adequate. The following is a summary of the principal results of the investigations.

When the I = B = R Research Home was being heated by a forced-circulation hot-water system using an oil-fired boiler vented to the inside chimney, the chimney efficiency — that is, the heat regained by the house from the chimney in percent of the total heat available in the chimney gases at the basement ceiling level — amounted to about 31 percent. Studies of masonry chimney performances at Battelle Memorial Institute and at the National Bureau of Standards gave results which were in close agreement with those obtained in the Research Home, even though there were differences in cross-sectional areas, total heights, and methods of operation of the various chimneys.

ABSTRACT (Concluded)

For any given value of chimney efficiency there is a direct relation between over-all house efficiency, combined boiler and smoke pipe efficiency, and the heat supplied to the house by the chimney in percent of the total heat utilized by the house.

The heat supplied to the house from the chimney may be sufficient to result in unequal air temperature distribution in the rooms unless an allowance for this heat is made in selecting the radiation for each room. It is suggested that the heat to be supplied by the installed radiation in a room should be reduced by an amount equal to 1.5 percent of the calculated heat loss of the house for each side of the chimney exposed to that room.

CONTENTS

SYMBOLS 7

I. INTRODUCTION 9

1. Preliminary Statement 9
2. Acknowledgments 9
3. Object of Investigation 10

II. EQUIPMENT 11

4. Research Home 11
5. Heating System 12
6. Chimney 15

III. TEST PROCEDURE 16

7. General Statement 16
8. Observations 16

IV. COMPUTATIONS USED IN FLUE GAS TEMPERATURE METHOD 18

9. General Statement 18
10. Average Temperatures and Draft During On-Periods 20
11. Average Rate of Flow During On-Periods 21
12. Average Temperatures and Draft During Off-Periods 23
13. Average Rate of Flow During Off-Periods 24
14. Heat Supplied to House from Chimney Gases, Daily 25
15. Heat Available in Chimney Gases at Basement Ceiling Level 26

V. COMPUTATIONS USED IN PLASTER SURFACE TEMPERATURE METHOD 27

VI. RESULTS 29

16. Heat Supplied to House from Chimney Gases, Using Flue Gas Temperature Method 29
17. Heat Supplied to House from Chimney Gases, Using Plaster Surface Temperature Method 29
18. Chimney Heat Transfer Efficiency 31
19. Heat Utilization 35

VII. Summary 39

APPENDIX A. HEAT UTILIZATION AND OVER-ALL HOUSE EFFICIENCY 41

APPENDIX B. APPLICATION OF PROPOSED DESIGN PROCEDURE TO RESEARCH HOME 44

APPENDIX C. CALCULATION OF DAILY TOTAL HEAT SUPPLIED TO HOUSE FROM THE CHIMNEY GASES 46

FIGURES

1. I=B=R Research Home 11
2. Floor Plans Showing Radiator Locations 12
3. Basement Plan with Location of Heating and Testing Equipment 13
4. Control System 14
5. Chimney Details 15
6. Characteristic Chimney Gas Temperatures and Draft Records 19
7. Dry Flue Gas per Pound of Oil Burned 22
8. Heat Supplied to House from Inside Chimney with Oil-Fired Boiler 30
9. Performance of Inside Chimney in I=B=R Research Home 33
10. Chimney Efficiencies Obtained from Three Investigations 34
11. Relationship Between Heat Obtained from Chimney and Operating Efficiencies 36
12. Temperature of Water at Top of Boiler for Three Operating Conditions 42
13. Over-all House Efficiency, Three Operating Conditions 42
14. Relationship Between Boiler Water Temperature and Over-all House Efficiency 43

TABLES

1. Values of Exponent n Used in Equations 13 and 14 24
2. Data on I=B=R Research Home Illustrating Use of Suggested Radiation Selection Procedure 45
3. Daily Heat Supplied to House from Chimney Gases, Using Flue Gas Temperature Method 46
4. Daily Heat Supplied to House from Chimney Gases, Using Plaster Surface Temperature Method 47

SYMBOLS

A = area of plaster wall exposed to rooms and enclosing chimney, sq ft
a_1 = area of plaster wall exposed to rooms and enclosing chimney on first story, sq ft
a_2 = area of plaster wall exposed to rooms and enclosing chimney on second story, sq ft
C_p = specific heat of dry chimney gases, 0.24 Btu per lb (F)
C_{ps} = specific heat of the water vapor in the chimney gases formed by the combustion of hydrogen in the fuel, 0.46 Btu per lb (F)
D = observed chimney draft at the level of the basement ceiling, in. of water
D_b = average chimney draft at the level of the basement ceiling, in. of water
D_m = chimney draft at the level of the basement ceiling at the end of the on-period, in. of water. This is the same as the draft at the start of the following off-period.
E_c = chimney efficiency
E_h = over-all house efficiency
E_u = combined boiler and smoke pipe efficiency
f_i = surface conductance, Btu per hr (sq ft) (F) — assumed = 1.65
H = total heat supplied to the house from chimney gases, Btu
H_b = heat available, in chimney gases at basement ceiling level, Btu
H_c = heat supplied to the house from water vapor formed by the combustion of hydrogen in the fuel, Btu
H_d = heat supplied to the house from dry chimney gases, Btu
H_f = total heat available in the fuel burned, Btu per hr
H_L = total heat utilized by the house, Btu per hr
H_2 = hydrogen in the fuel, percent by weight
h_1 = heat supplied to first story rooms from chimney gases, Btu per hr
h_2 = heat supplied to second story rooms from chimney gases, Btu per hr
N = number of burner cycles per day
p = density of chimney gases at the level of the attic floor, lb per cu ft
Q_c = heat obtained by the house from the chimney gases divided by the heat utilized by the house
t = observed temperature of chimney gases at the level of the attic floor, F

t_a = average room air temperature, F

t_b = average temperature of the chimney gases at the level of the basement ceiling, F

t_c = average temperature of chimney gases at the level of the attic floor, F

t_m = temperature of chimney gases at the level of the attic floor at the end of on-period, F

t_p = temperature of chimney gases at the level of the basement ceiling at the end of the on-period, F. This is the same as the temperature at the start of the following off-period.

t_s = average surface temperature of plaster wall exposed to rooms and enclosing chimney, F

t_1 = average surface temperature of a_1, F

t_2 = average surface temperature of a_2, F

t_3 = average room air temperature of first story, F

t_4 = average room air temperature of second story, F

Δt = indoor-outdoor temperature difference, F

V = velocity of chimney gases, ft per sec

W = rate of flow of dry chimney gases, lb per hr

W_d = average rate of flow of dry chimney gases, lb per hr

W_o = weight of oil burned, lb per hr

Φ = time, hr

ϕ = time from start of any given on-period or off-period, min

ϕ_2 = duration of any given on-period or off-period, min

I. INTRODUCTION

1. Preliminary Statement

This is the eighth bulletin to be published under a cooperative agreement between the Institute of Boiler and Radiator Manufacturers and the University of Illinois. This agreement was formally approved January 2, 1940. Under the terms of the agreement the Institute is represented by an Advisory Research Committee of five members whose function is to propose such problems for investigation as are of the greatest interest to the manufacturers and installers of steam and hot-water heating equipment. Of these problems, the Engineering Experiment Station staff selects for study those which can best be investigated with the facilities and equipment available at the University. The Institute provides funds for defraying a major part of the expense of this research work.

From January 1941 to the Spring of 1945 the I = B = R Research Home was used continuously in studies on hot-water heating systems, and during the 1945-46 season tests were made on a one-pipe steam system. In all these studies it was observed that a large part of the total heat required to offset the heat loss of the Research Home was obtained from sources other than the radiators. In a previous bulletin[1] a discussion is given as to the amounts of heat supplied to the house by the occupants and from the use of electricity and gas in the house. In that bulletin no attempt was made to estimate the amount of heat supplied to the house from the chimney, although it was acknowledged that some useful heat was supplied from this source.

The present bulletin presents a discussion of the useful heat supplied to the I = B = R Research Home from the inside chimney when the house was being heated by an oil-fired, forced-circulation, hot-water heating system. The data on which this discussion is based were largely obtained during the winters of 1941-42 and 1942-43.

2. Acknowledgments

The results presented in this bulletin were obtained in connection with a cooperative investigation sponsored jointly by the Engineering Experiment Station of the University of Illinois and the Institute of

[1] "Performance of a Hot-Water Heating System in the I=B=R Research Home at the University of Illinois," Univ. of Ill. Eng. Exp. Sta. Bul. 349, Chap. VIII, Sect. 26.

Boiler and Radiator Manufacturers. The investigation has been carried on as a project of the Department of Mechanical Engineering, and was conducted under the general administrative direction of Emeritus Dean M. L. Enger, then Director of the Engineering Experiment Station, and of Emeritus Professor O. A. Leutwiler, Head of the Department of Mechanical Engineering. Acknowledgment is hereby made to various manufacturers who cooperated by furnishing materials and equipment used in the investigation.

3. Object of Investigation

The object of this investigation was to determine the quantity of heat liberated to the rooms of the Research Home from the inside chimney which was being used as the vent for the oil-fired, hot-water heating system.

II. EQUIPMENT

4. Research Home

The Research Home shown in Figs. 1 and 2 and described in detail in Engineering Experiment Station Bulletin 349 is a two-story building typical of the small, well-built American home. The construction is brick veneer on wood frame, and all outside walls and the second-story ceiling are insulated with mineral wool bats $3\frac{5}{8}$ in. thick. A vapor barrier placed between the studs and the plaster base prevents condensation on the sheathing by retarding the passage of water vapor from the rooms into the insulation in the walls. The calculated coefficient of heat transmission, U, for the wall section is 0.074 Btu per hr (sq ft) (F). All windows and the two outside doors are weatherstripped. Two storm doors were used. The total calculated heat loss under design conditions of -10 F outdoors and 70 F indoors is 43,370 Btu per hr for the house, excluding the basement.

Fig. 1. I=B=R Research Home

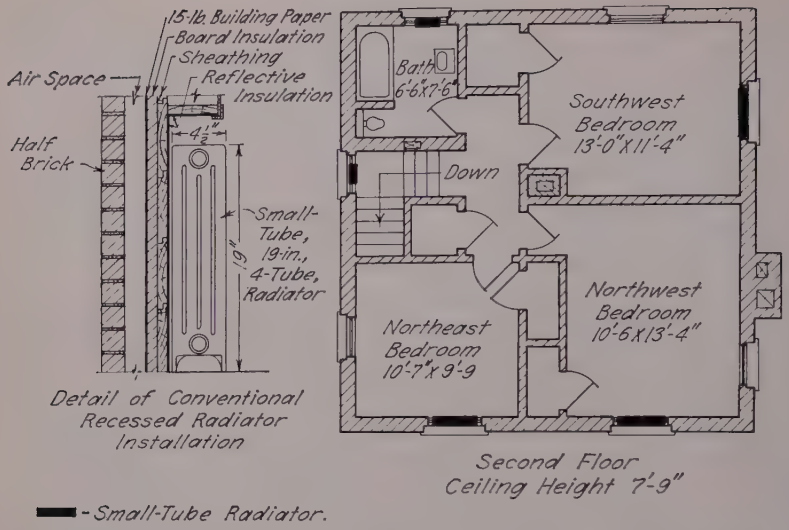

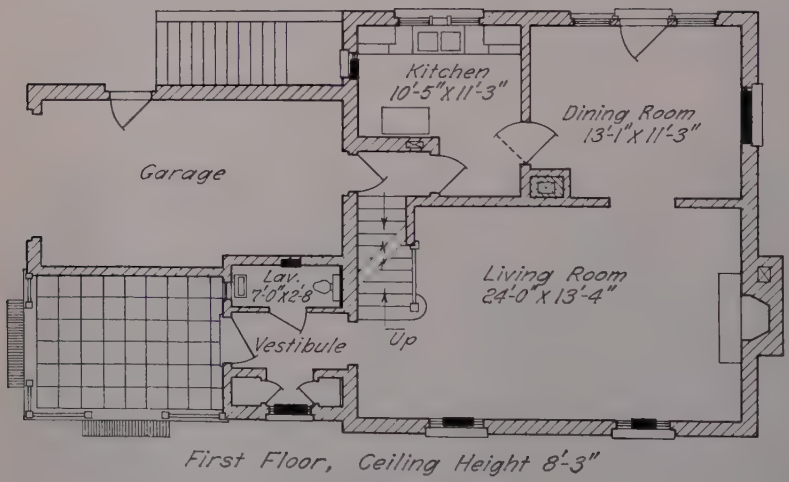

Fig. 2. Floor Plans Showing Radiator Locations

5. Heating System

An oil-fired, cast-iron boiler used in connection with a one-pipe, forced-circulation, hot-water heating system was used in the Research Home during the heating seasons of 1941-42 and 1942-43. Small-tube type, 19-in., 4-tube, cast-iron radiators set in open recesses below windows were used to transfer the heat from the boiler water to the room air. In each case there was about 4 in. of clearance between the ends of the radiator and the sides of the recess, 2¼ in. between the top of the

radiator and the top of the recess, and ¼ in. between the back of the radiator and the wall of the recess. The front of the radiator was approximately flush with the wall of the room. The radiators were connected to two supply loops located in the basement as shown in Fig. 3. The locations of radiators in each room of the house are shown by the black rectangles in Fig. 2.

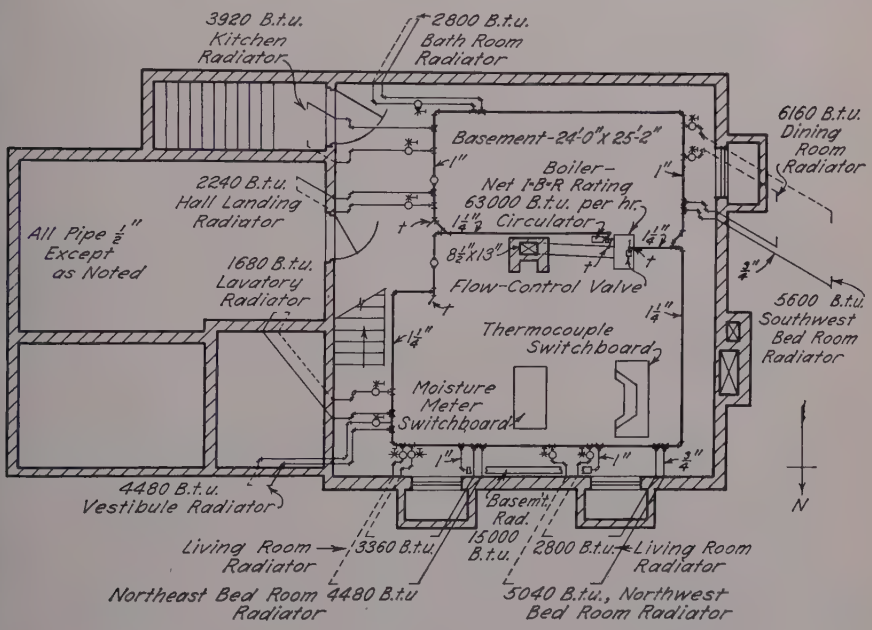

Fig. 3. Basement Plan with Location of Heating and Testing Equipment

The amount of radiation installed in each room was based on a heat emission rate of 200 Btu per sq ft of equivalent direct radiation with a mean water temperature of 195 F and a 10 F drop through the radiator, and was sufficient to offset the calculated heat loss at an outdoor temperature of −10 F with the circulator operating continuously. In selecting the radiators the rating of 1.6 sq ft E.D.R. per section of free standing radiation, as listed in the manufacturer's catalog, was reduced by 12.5 percent in order to compensate for the anticipated reduction in heat output of the radiators when installed in recesses.

The cast-iron, hot-water boiler was composed of three 4-in. sections insulated on the front, back, sides, and top by a mineral wool blanket 1 in. in thickness, and was completely enclosed with an enameled sheet-metal jacket. All cracks around the base of the boiler and between

sections were sealed with asbestos cement to prevent leakage of air into, or products of combustion out of, the boiler. The boiler had a net I = B = R rating of 63,000 or a gross I = B = R output of 95,000 Btu per hr when fired with oil at the rate of 1.0 gal per hr. The oil burner was of the pressure atomizing, conversion type, and the refractory combustion chamber was 11 in. wide by 12 in. long by 12½ in. high, inside dimensions. The system was equipped with a 1¼-in. circulator and an angle flow-control valve.

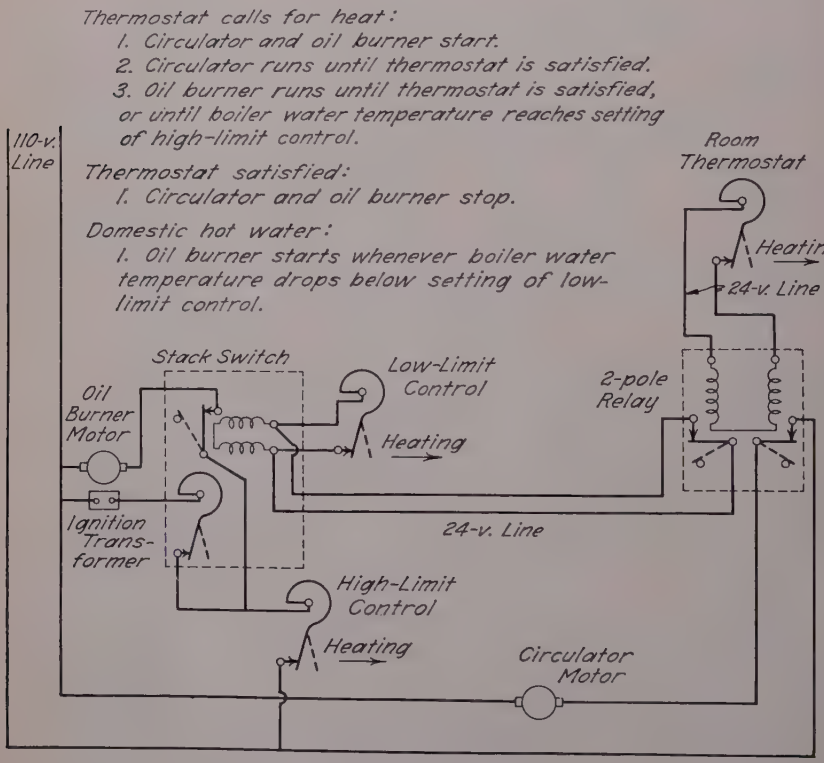

Fig. 4. Control System

The operation of the burner and circulator was regulated by means of a conventional set of controls consisting of a room thermostat which was located in the living room, an electric clock with a self-contained time switch, a high-limit control, a stack switch, and a relay. The stack switch was connected in the burner circuit, and served as a safety control in case of failure of the ignition or oil supply. The room thermostat was of the heat-anticipating type. The high-limit control, attached

to the surface of the supply trunk immediately above the top of the boiler, served as an additional safety control to prevent overheating the water in the boiler. A diagram of the control system and the sequence of operations are shown in Fig. 4.

6. Chimney

The chimney to which the boiler was connected had a height of 35 ft 2 in. measured from the basement floor and consisted of a 6½-in.-by-11-in. fireclay flue lining enclosed by one course of red brick. The chimney extended up through the central part of the house so that it was completely surrounded by heated space from its base to the level of the second story ceiling. There was no direct contact between the chimney and any of the house framing. The plaster walls were separated from the masonry by an air space averaging about 5 in. in width. At the second story and basement ceiling levels this space was packed with mineral wool to prevent the circulation of air between the space around the chimney and the attic or basement. The location of the draft regulator and thermocouples, and details of the chimney construction and flue connection, are shown in Fig. 5.

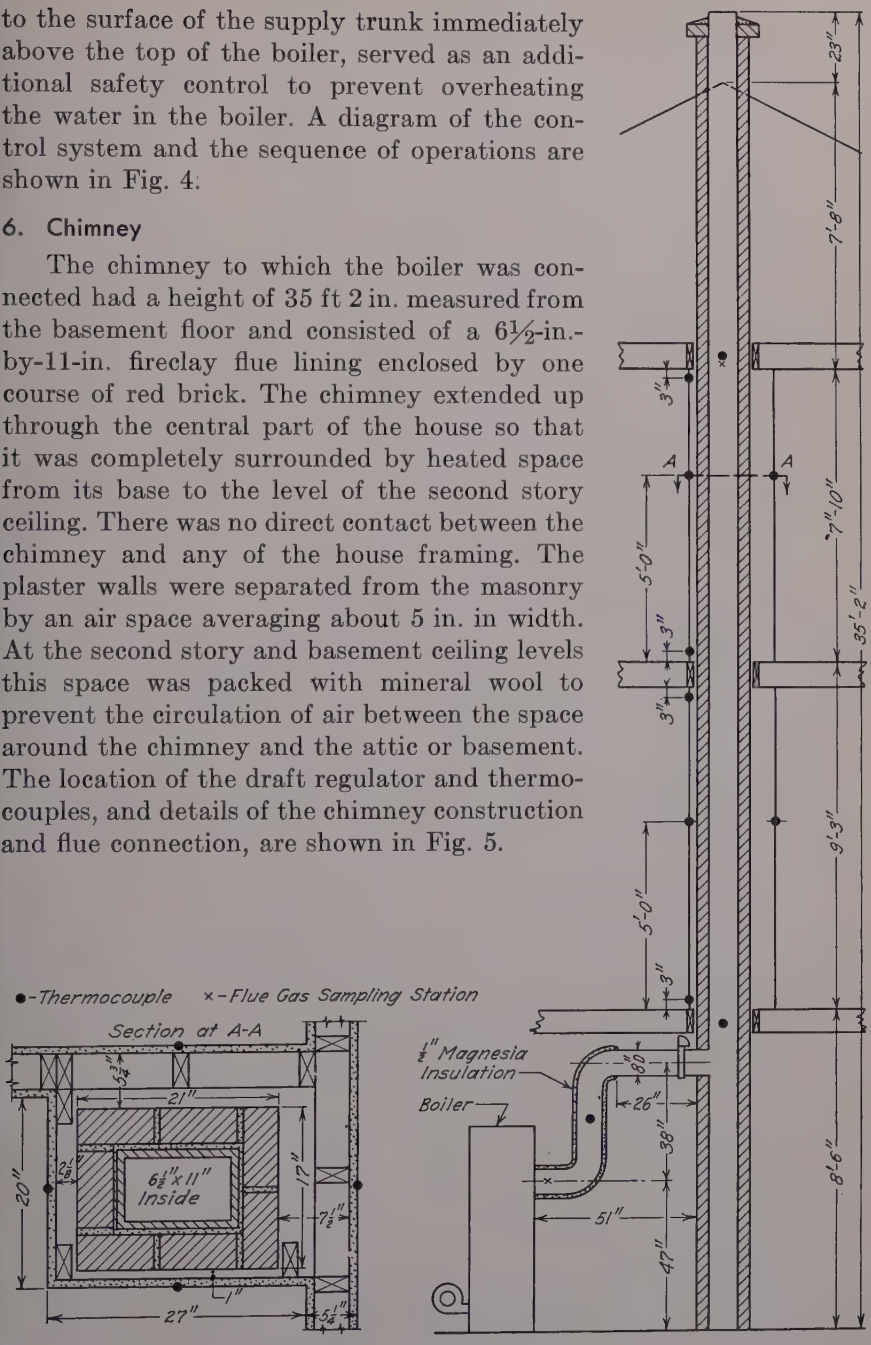

Fig. 5. Chimney Details

III. TEST PROCEDURE

7. General Statement

The tests included in this discussion were made while operating the house on series B during the heating season of 1941-42.[1] In this series the flow control valve was locked open so that water could circulate by gravity to the radiators during the off-period. The burner and circulator operation was controlled by the room thermostat alone, with no provision made for heating domestic hot water. An oil burning rate of 1.1 gal per hr was used. This rate was the minimum obtainable with a clean fire and with a CO_2 content of the flue gases not less than 8 percent at the smoke outlet of the boiler. The oil used weighed 7 lb per gal and had a calorific value of 19,550 Btu per lb. In order to keep a constant draft on the boiler at all times, a draft regulator was installed in the flue pipe connecting the boiler to the chimney.

During all tests the temperature of the air 30 in. above the floor in the heated portion of the house was maintained constant at approximately 72 F both day and night. The windows, including those in the bedrooms, remained closed at all times.

8. Observations

To obtain the data necessary for the computations of the heat supplied to the house from the chimney, the following observations were made.

(a) *Chimney Gas Temperatures.* A continuous record was made of the temperatures of the chimney gases at the levels of the attic floor and the basement ceiling and of the temperature of the gases at the smoke outlet of the boiler. The locations of these temperature measuring stations are shown in Fig. 5. These temperatures were measured by means of thermocouples made of chromel-alumel 22 B and S gage wire and connected to a recording type, multi-point potentiometer.

(b) *Available Draft in the Chimney.* A continuous record was made of the available draft in the chimney at the level of the basement ceiling. The draft recorder used for this purpose was readable to 0.01 in. of water.

[1] For full details of this operating procedure see "Performance of a Hot-Water Heating System in the I=B=R Research Home at the University of Illinois," Univ. of Ill. Eng. Exp. Sta. Bul. 349, pp. 19–21.

(c) *Flue Gas and Chimney Gas Analyses.* Gas sampling stations were located in the smoke outlet of the boiler and at the level of the attic floor. A continuous record was made of the CO_2 at the smoke outlet by means of a recording CO_2 analyzer. The CO_2 content of the chimney gases at the level of the attic floor was measured with an Orsat apparatus.

(d) *Rate of Flow of Chimney Gases During On-Period.* This rate of flow was obtained by direct calculation from chimney gas and fuel analyses. The calculation procedure is explained in detail in Section 11.

(e) *Rate of Flow of Chimney Gases During Off-Periods.* This rate of flow was obtained by a CO_2 dilution method as explained in Section 13.

(f) *Plaster Surface Temperatures.* The surface temperatures of the plaster on the inside walls surrounding the chimney were observed daily at 7:00 am., 11:00 a.m., 5:00 p.m., and 10:00 p.m. The locations of the thermocouples used are shown in Fig. 5.

(g) *General Observations.* At 7:00 a.m., 11:00 a.m., 5:00 p.m., and 10:00 p.m. observations were recorded of the temperature of the air in each room at 3 in., 30 in., and 60 in. above the floor, and 3 in. below the ceiling; the temperature of the air in the basement and in the attic; and the relative humidity in the rooms. Complete daily records were made of the weight of oil consumed and of the operating time, the number of cycles, and the power consumption of the oil burner and circulator. Continuous records were made of the temperature of the water at the boiler outlet and return, and of the outdoor air temperature. Other daily observations included the total amount of electricity and gas used in the house, the number of occupants, and general weather conditions.

IV. COMPUTATIONS USED IN FLUE GAS TEMPERATURE METHOD

9. General Statement

The heat supplied to the heated portion of the house from chimney gases may be divided into three parts: (1) the heat obtained from the dry chimney gases, (2) the heat obtained from the water vapor in the chimney gases formed by the combustion of hydrogen in the fuel, and (3) the heat obtained from the water vapor in the chimney gases carried in by the air for combustion.

Based on the assumption that all the heat given up by the flue gases while passing from the level of the basement ceiling to the level of the attic floor is transmitted to the heated portion of the house, the heat supplied to the house from the dry chimney gases may be computed from the equation:

$$H_d = W_d C_p (t_b - t_c) \Phi \qquad (1)$$

H_d = heat supplied to the house from the dry chimney gases, Btu
W_d = average rate of flow of the dry chimney gases, lb per hr
C_p = specific heat of chimney gases, 0.24 Btu per lb (F)
t_b = average temperature of the chimney gases at the level of the basement ceiling, F
t_c = average temperature of the chimney gases at the level of the attic floor, F
Φ = time, hr

The heat supplied to the house from the water vapor in the chimney gases formed by the combustion of hydrogen in the fuel may be computed from the equation:

$$H_c = 0.09\, W_o\, H_2\, C_{ps} (t_b - t_c) \Phi \qquad (2)$$

where

H_c = heat supplied to the house from water vapor formed by the combustion of hydrogen in the fuel, Btu
W_o = weight of oil burned, lb per hr
H_2 = hydrogen in the fuel, percent by weight
C_{ps} = specific heat of the water vapor, 0.46 Btu per lb (F)
t_b, t_c, and Φ = same as in Eq. 1

In addition to the water vapor resulting from the combustion of hydrogen in the fuel, about 0.005 lb of water vapor were supplied with

each pound of basement air admitted to the system. The heat regained from the water vapor in the air for combustion was less than 1.0 percent of the total heat regained and therefore was neglected in all calculations.

The rate of flow of chimney gases was not continuous and uniform, and it was not possible to calculate the rate of flow during the off-periods from the analyses of the fuel and chimney gases as was possible for the on-periods. Hence it was immediately evident that in order to use Eqs. 1 and 2 to calculate the amount of heat transmitted to the house from the flue gases over the period of a day, the on-periods and the off-periods would have to be treated separately.

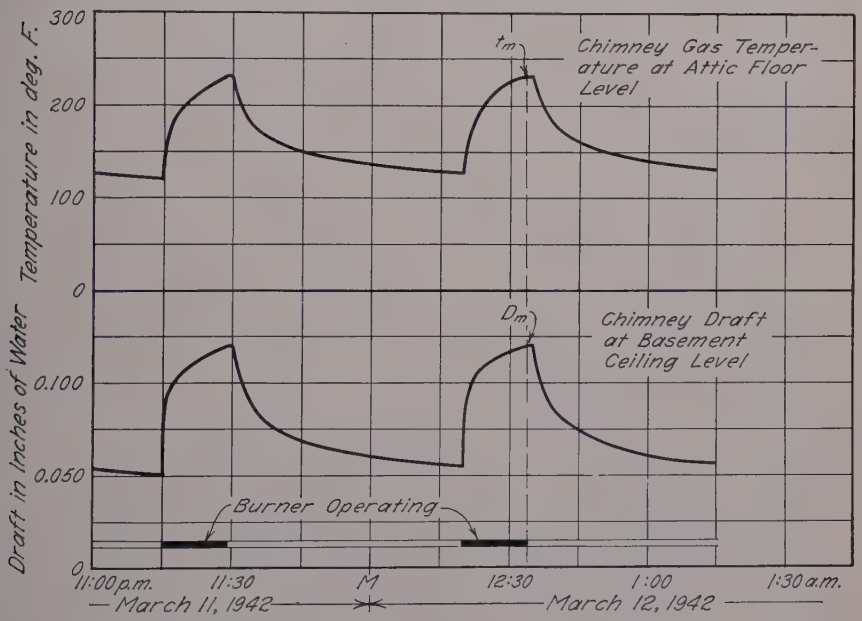

Fig. 6. Characteristic Chimney Gas Temperatures and Draft Records

Continuous records were made of the available draft in the chimney at the level of the basement ceiling, and the temperature of the chimney gases at the levels of the basement ceiling and the attic floor. The characteristic shapes of the temperature and draft records are shown in Fig. 6. The shapes of these curves for both the on- and the off-periods were such that no direct method of averaging could be used; however, by integrating a large number of characteristic curves, it was found that the average temperature and average draft for a given on- or off-period could be expressed in terms of the maximum temperature or

draft shown by the recorder chart for that period. Furthermore, since the rate of flow of the chimney gases is a function of the draft, the average rate of flow could be determined from the average draft. The methods used to obtain the separate averages for the on-periods and off-periods from which the heat losses in the dry chimney gases were computed are explained in Sections 10–13. The total heat transmitted during any given day was then obtained by taking the sum of the heat transfers computed for the individual cycles occurring during that day.

10. Average Temperatures and Draft During On-Periods

For a large number of characteristic on-periods the temperatures of the chimney gases at the level of the attic floor as read from the recorder charts were plotted against time on logarithmic paper. The resulting curves were straight lines, all having practically the same slope. The average slope was 0.14 and the characteristic equation was of the form:

$$t = C\phi^{0.14} \tag{3}$$

in which

ϕ = time from start of on-period, min
t = instantaneous temperature of the chimney gases at the level of the attic floor at the time ϕ, F
C = a constant

Integrating Eq. 3 between the limits of zero and ϕ_2 and dividing by ϕ_2:

$$t_c = \frac{C\,\phi_2^{0.14}}{1.14} \tag{4}$$

in which

t_c = average temperature of the chimney gases at the level of the attic floor, F
ϕ_2 = duration of on-period, min

From Eq. 3 the temperature, t_m, at the end of the on-period is

$$t_m = C\,\phi_2^{0.14} \tag{5}$$

in which

t_m = temperature of chimney gases at the level of the attic floor, F

Dividing Eq. 4 by Eq. 5

$$t_c = \frac{t_m}{1.14} = 0.877\,t_m \tag{6}$$

Equation 6 gives the relation between the average temperature for the on-period and the temperature attained at the end of the on-period. Since the latter was always the maximum temperature attained in the given cycle, it could be read from the chart with considerable accuracy.

By a similar analysis it was found that the average temperature of the chimney gas at the level of the basement ceiling could be obtained by using the equation:

$$t_b = 0.901\, t_p \tag{7}$$

in which

t_b = average temperature of the chimney gases at the level of the basement ceiling, F

t_p = temperature of the chimney gases at the level of the basement ceiling at end of the on-period, F

t_p was obtained directly from the recorder chart.

Likewise, the average draft at the level of the basement ceiling could be obtained from the recorder charts by using the equation:

$$D_b = 0.917\, D_m \tag{8}$$

in which

D_b = average draft, in. of water

D_m = draft at end of on-period, in. of water

11. Average Rate of Flow During On-Periods

For a large number of on-periods, and over a wide range of chimney temperatures, a series of observations were made of the percentage of CO_2 in the chimney gases at the level of the attic floor and the draft in the chimney just above the point at which the smoke pipe entered the chimney. From these CO_2 readings, made by means of an Orsat apparatus, the corresponding rates of flow of the chimney gases in pounds per hour were computed from the curves shown in Fig. 7. These curves were obtained[1] by assuming different percentages of excess air and calculating the resulting CO_2 and weights of the products of combustion from the analysis of an oil typical of that used for the tests reported in this bulletin. From the weight rates of flow, the velocities of the gases in the chimney were computed and plotted on log paper against the corresponding observed drafts. The resulting curve was a straight line represented by the equation:

$$V = 1.71 \sqrt{\frac{D}{p}} \tag{9}$$

in which

V = velocity of chimney gases, ft per sec

D = draft at the level of the basement ceiling, in. of water

p = density of chimney gases at the level of the attic floor, lb per cu ft

[1] "Combustion Efficiencies as Related to Performance of Domestic Heating Plants," Univ. of Ill. Eng. Exp. Sta. Circ. 44, 1942, pp. 21—23.

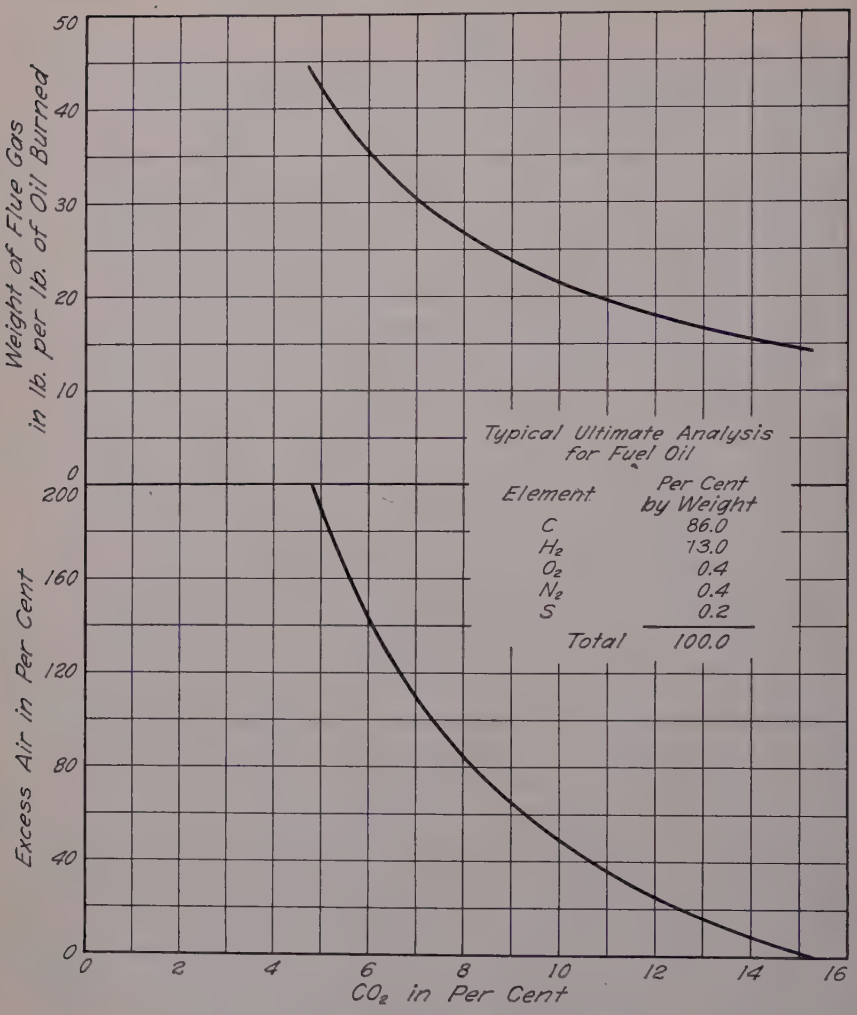

Fig. 7. Dry Flue Gas per Pound of Oil Burned

This was regarded as the characteristic flow equation applying to this chimney and to the measurements made at the points previously specified. Expressing the velocity in terms of weight of gases flowing in pounds per hour and the density in terms of the temperature of the gases, Eq. 9 reduces to

$$W = 20{,}200 \sqrt{\frac{D}{t + 460}} \tag{10}$$

in which

W = weight of dry chimney gas, lb per hr
D = observed draft at the level of the basement ceiling, in. of water
t = temperature of chimney gases at the level of the attic floor, F

The average rate of flow of the chimney gases for any given on-period, W, was determined from Eq. 10 by substituting for t the average temperature of the chimney gases at the level of the attic floor as determined by Eq. 6 and for D the average draft at the level of the basement ceiling as determined by Eq. 8.

12. Average Temperatures and Draft During Off-Periods

By an analysis similar to that discussed in Section 10, it was found that the average temperature of the chimney gas at the level of the attic floor during any given off-period could be expressed by the equation:

$$t_c = \frac{t_m}{0.814\ \phi_2^{0.145}} \tag{11}$$

in which

t_c = average temperature of the chimney gases at the level of the attic floor, F
t_m = temperature of the chimney gases at the level of the attic floor at the start of the off-period, F. This is equal to t_m for the preceding on-period.
ϕ_2 = length of off-period, min

Likewise, the average temperature of the chimney gas at the level of the basement ceiling, t_b, was expressed by the equation:

$$t_b = \frac{1.13\ t_m}{\phi_2^{0.23}} \tag{12}$$

in which t_m and ϕ_2 are the same as in Eq. 11.

Draft curves similar to the temperature curves discussed in Section 10 were plotted and from these curves the characteristic equation was found to be of the form:

$$D = D_m\ \phi^n \tag{13}$$

in which

ϕ = time from start of off-period, minutes
D = observed chimney draft at the level of the basement ceiling at time ϕ, in. of water

D_m = chimney draft at the level of basement ceiling at the start of off-period, in. of water. This is the same as the draft at the end of the preceding on-period.

However, the exponent n in Eq. 13 was variable, the value being dependent on D_m as shown in Table 1.

Table 1
Values of Exponent n Used in Equations 13 and 14

D_m in. of water	n	D_m in. of water	n
0.100	−0.297	0.140	−0.151
0.110	−0.230	0.150	−0.136
0.120	−0.193	0.160	−0.123
0.130	−0.170	0.170	−0.114

Integrating Eq. 13 between the limits of zero and ϕ_2 and dividing by ϕ_2

$$D_b = \left(\frac{\phi_2{}^n}{n+1}\right) D_m \qquad (14)$$

in which

D_b = average chimney draft at the level of the basement ceiling, in. of water
ϕ_2 = length of the off-period, min
D_m = the same as in Eq. 13

13. Average Rate of Flow During Off-Periods

During the off-periods no combustion occurred and air was drawn through the burner and over the heating surfaces in the boiler by the action of the draft in the chimney. Since there was no primary heat source, this draft was created entirely by the residual heat in the combustion chamber, boiler and chimney. Furthermore, since no CO_2 was generated, it was not possible to determine from the analyses of the gases and fuel the weight of gases flowing, as was done for the on-period. Therefore, some other method had to be selected.

The method employed was to introduce CO_2 into the chimney at a predetermined constant rate, and to measure the concentration of CO_2 appearing at the level of the attic floor. For this purpose pure CO_2 was stored in a gasometer and introduced into the base of the chimney through a short length of horizontal pipe extending across the chimney and perforated on both sides. The gasometer afforded a means of both measuring and controlling the rate of flow of CO_2. The perforated pipe introduced the CO_2 horizontally and at a sufficiently low velocity to permit diffusion across the whole cross sectional area of the chimney. It also eliminated the possibility of any injection action interfering with the normal draft. Sufficient CO_2 was introduced to produce a

concentration of about 2 percent at the level of the attic floor, as measured by means of an Orsat apparatus. From this concentration the rate of flow of the chimney gases during the off-periods was determined with an accuracy of ± 5 percent. From the rates of flow so determined, the velocities of the chimney gases were computed and plotted on logarithmic paper against the corresponding observed drafts as was done for the on-periods. The characteristic flow equation in this case was of the form:

$$V = 1.26 \sqrt{\frac{D}{p}} \qquad (15)$$

in which

V = velocity of chimney gases, ft per sec
D = observed chimney draft at the level of the basement ceiling, in. of water
p = density of chimney gases at the level of the attic floor, lb per cu ft

Expressing the velocity in terms of weight of gases flowing in pounds per hour and the density in terms of the temperature of the gases, Eq. 15 reduces to

$$W = 14{,}920 \sqrt{\frac{D}{t + 460}} \qquad (16)$$

in which

W = rate of flow of dry chimney gases, lb per hr
t = observed temperature of chimney gases at the level of the attic floor
D = the same as in Eq. 15

The average rate of flow of chimney gases for any given off-period, W_d, was determined from Eq. 16 by substituting for t the average temperature of the chimney gases at the level of the attic floor as determined by Eq. 11, and for D the average draft at the level of the basement ceiling as determined by Eq. 14.

14. Heat Supplied to House from Chimney Gases, Daily

The heat transmitted to the house from the dry flue gas, H_d, during each on- and off-period of the burner may be obtained by substituting in Eq. 1 the proper values of W_d, t_b, and t_c as derived in Sections 10 and 13 and substituting for Φ the duration of this on- or off-period, ϕ_2. The total heat transmitted to the house per day from the dry chimney gas is the summation of the heat transmitted during each on- or off-period occurring during that day.

To obtain the total heat transfer from the chimney gas to the house it is necessary to add to the total heat transfer from the dry flue gas, the heat obtained from the water vapor formed by the combustion of hydrogen, H_c. Heat is obtained from this source during on-periods of the burner only, and may be computed by substituting in Eq. 2 the values of t_b and t_c as derived in Section 10, the length of the on-period for Φ, and the proportionate weight of oil burned during the on-period for W_o. For the oil used in these tests, H_2 in Eq. 2 was equal to 13.0 percent. The heat obtained from the water vapor for any given day is the sum of the quantities of heat obtained during each individual on-period occurring during that day. The total heat obtained from the chimney gases, H, is the sum of the heat obtained from the dry flue gas plus that obtained from the water vapor formed by the combustion of hydrogen in the fuel. Detailed calculations of the total heat obtained from the chimney gas as determined by the flue gas temperature method are shown in Table 3, Appendix C.

Due to the relative locations of the temperature and flow measurement stations and of the draft regulator, the preceding computations include the effects of any basement air that has been introduced to the system through the draft regulator.

15. Heat Available in Chimney Gases at Basement Ceiling Level

The heat available in the chimney gases at the basement ceiling level, H_b, is the heat obtainable from these gases if cooled to room temperature. Therefore the heat available may be computed with the procedures given in Section 14 by substituting the average room temperature, t_a, for the average temperature of the chimney gases at the level of the attic floor, t_c.

V. COMPUTATIONS USED IN PLASTER SURFACE TEMPERATURE METHOD

A second method used in computing the total heat supplied to the house from the chimney gases was based on the observed surface temperature of the plaster walls around the chimney and the room air temperatures. In making these calculations use was made of the equation:

$$H = \Phi A f_i (t_s - t_a) \tag{17}$$

in which

H = total heat supplied to the house from the chimney gases, Btu
A = area of plaster wall exposed to rooms and enclosing chimney, sq ft
f_i = surface conductance, Btu per hr (sq ft) (F)—assumed = 1.65
t_s = average surface temperature of plaster wall exposed to rooms and enclosing chimney, F
t_a = average room air temperature, F
Φ = time, hr

Since there were slight differences in both the air and plaster surface temperatures for the first and second stories, the heat transfer was computed for each story separately as follows:

$$h_1 = \Phi a_1 f_i (t_1 - t_3) \tag{18}$$

$$h_2 = \Phi a_2 f_i (t_2 - t_4) \tag{19}$$

$$H = h_1 + h_2 \tag{20}$$

in which

h_1, h_2 = heat supplied to first and second story rooms from chimney gases, respectively, Btu
a_1, a_2 = areas of plaster wall exposed to rooms enclosing chimney on first and second stories, respectively, sq ft
t_1, t_2 = average surface temperatures of a_1 and a_2 respectively, F
t_3, t_4 = average room air temperatures of first and second stories respectively, F
f_i, Φ = same as in Eq. 17

The average room air temperature of the first story, t_3, was taken as the average of the air temperature readings observed each day at

the 60-in. level in the living room, dining room, and kitchen. Likewise, t_4 was taken as the average of the readings observed each day of the room air temperature at the 60-in. level in the three bedrooms.

In calculating the total daily heat supplied to the rooms from the chimney, Eqs. 18 and 19 may be further simplified by combining all constant terms to:

$$h_1 = C_1 (t_1 - t_3) \tag{21}$$

$$h_2 = C_2 (t_2 - t_4) \tag{22}$$

in which

$$C_1 = a_1 f_i \Phi = 81 \times 1.65 \times 24 = 3208$$
$$C_2 = a_2 f_i \Phi = 72.8 \times 1.65 \times 24 = 2887$$

Detailed calculations of the total heat supplied to the house by the chimney gases as determined by the plaster surface temperature method are shown in Table 4, Appendix C.

VI. RESULTS

16. Heat Supplied to House from Chimney Gases, Using Flue Gas Temperature Method

In Fig. 8 curve 1 shows the daily heat supplied to the house from the chimney as determined by measurements of flue gas temperatures and quantities. The test points are quite scattered, as is to be expected because the coordinates selected imply that the heat transfer is a function only of indoor-outdoor temperature difference. Actually it is a function of total burner operating time, boiler water temperature, and intensity of draft, all of which are affected by the amount of sunshine and average wind velocity as well as the indoor-outdoor temperature difference. Since the test observations did not make it possible to isolate the effects of wind and sunshine, sufficient tests were run to permit drawing a curve representing "average" conditions.

Curve 3 of Fig. 8 represents the heat supplied to the house from the chimney as determined by measurements of flue gas temperatures and quantities, expressed in percent of the total heat loss of the house. Curve 3 was obtained by multiplying values read from curve 1 by 100 and dividing by the actual heat loss of the house for the corresponding indoor-outdoor temperature difference. The actual heat loss was obtained by measurement of all heat supplied to the residence.[1]

From curve 3, Fig. 8, it may be observed that as the indoor-outdoor temperature difference increased up to about 25 F there was a sharp increase in the useful heat obtained from the chimney when expressed in percent of the total heat loss of the house. Above an indoor-outdoor temperature difference of 25 F this increase was less pronounced, ranging from 13.5 percent to a maximum of 14 percent. At an indoor-outdoor temperature difference of 34 F (representative of average winter temperatures in Urbana, Illinois) the heat supplied to the house from the chimney as computed by the flue gas method amounted to 14.0 percent of the total heat loss of the house.

17. Heat Supplied to House from Chimney Gases, Using Plaster Surface Temperature Method

The useful heat obtained from the chimney each day as computed from the observed plaster surface and room air temperature is shown

[1] For a discussion of the actual heat loss of the I=B=R Research Home see Section 26 of "Performance of a Hot-Water Heating System in the I=B=R Research Home at the University of Illinois," Eng. Exp. Sta. Bul. 349.

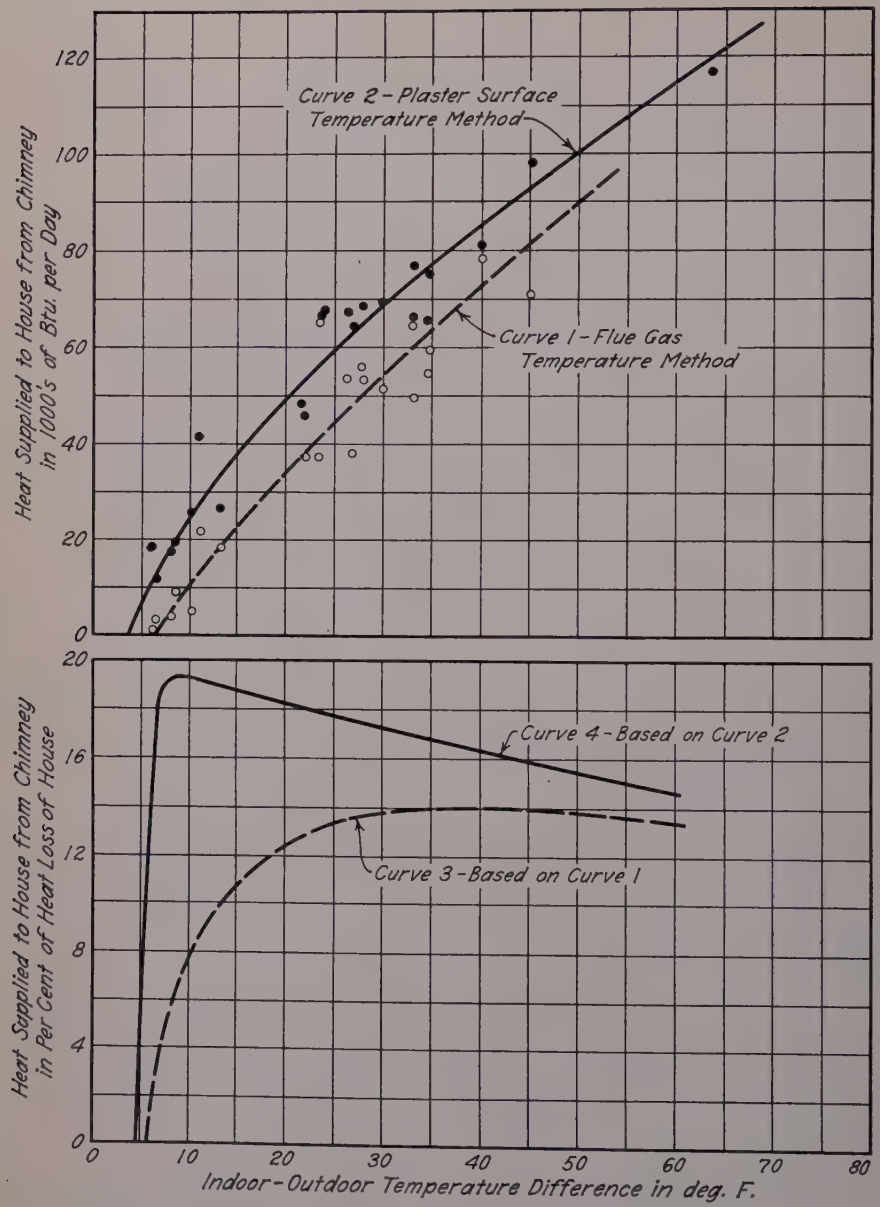

Fig. 8. Heat Supplied to House from Inside Chimney with Oil-Fired Boiler

by curve 2 of Fig. 8. The test points for curve 2 are for the same days as those for curve 1, and supposedly would have identical values if both methods of calculation were exact. However, both methods of computation are subject to unavoidable inaccuracies. The formulas for obtaining the average flue gas temperature and average rate of flow as given in Sections 9–13 are approximate and are influenced by variations in wind and sunshine, whereas these variations do not greatly influence the plaster surface temperature. Therefore, the plaster surface temperature method is probably the more accurate method of calculating the heat supplied to the house from the chimney. The difficulties involved in this method were to obtain the true average plaster surface and ambient air temperatures, and to select the proper plaster area, since (as shown in Fig. 5) some of the walls around the chimney were continuous with intermediate partitions in the house. In this analysis it was assumed that only the wall area actually surrounding the chimney was involved.

The correlation of the test points for curve 2 in Fig. 8 is better than that for curve 1 and, as indicated in the preceding paragraph, there is reason to believe that these points more accurately represent actual conditions.

Curve 4, based on curve 2, was obtained in the same manner as curve 3, which was described in Chapter V. This curve indicates that as soon as the outdoor temperature dropped low enough to require some heat in the house the useful heat obtained from the chimney expressed in percent of the total heat loss of the house rose very sharply, from 0 to 19.5 percent. As the indoor-outdoor temperature difference increased beyond this point the ratio of the heat obtained from the chimney to the heat loss of the house steadily decreased to a value of about 14.7 percent at an indoor-outdoor temperature difference of 60 F. At a temperature difference of 34 F the useful heat obtained from the chimney as computed from observed plaster surface and ambient air temperature was about 17 percent of the actual heat loss of the house, as compared to the value of 14.0 percent obtained by using observed flue gas temperatures and rates of flow in computing the useful heat obtained from the chimney.

18. Chimney Heat Transfer Efficiency

The heat supplied to the house from the inside chimney may be expressed as a percentage of the heat available in the chimney gases

at the basement ceiling level. Since this value represents the heat transferred as related to the initial heat available, it has been designated "Chimney Heat Transfer Efficiency" or simply "Chimney Efficiency." The chimney efficiency has been determined over a range of indoor-outdoor temperature differences by means of observed rates of flow of the chimney gases and the temperatures of the chimney gases at the basement and second story ceiling levels. A plot of these chimney efficiencies together with the average flow rates and temperatures of the chimney gases at the basement ceiling level is shown in Fig. 9. The chimney efficiency is fairly constant over a wide range of indoor-outdoor temperature differences, and is equal to 31 percent at an indoor-outdoor temperature difference of 34 F (representative of average winter temperatures in Urbana, Illinois).

In addition to the investigation reported in this bulletin, studies of the performance of residential chimneys have been made at the National Bureau of Standards[1] and at Battelle Memorial Institute.[2] All studies were limited to masonry chimneys; however, as shown in Fig. 10, there were variations in the physical dimensions of the chimneys, the method of operation, and the type of fuel used. While the total height of the chimneys differed, it should be noted that the heights between temperature measuring stations used for computing the chimney efficiency were approximately equal.

The principal object of the investigation at both Battelle and the Bureau of Standards was to study the draft characteristics of residential chimneys at various gas flow rates and inlet temperatures. The procedure adopted for both of these investigations was to heat the chimney gases to the desired temperature using gas or electricity as the source of heat and to regulate the rate of gas flow into the base of the chimney by means of a damper.

The tests in the Research Home were made while studying the performance characteristics of an oil-fired, forced-circulation, hot-water heating system operating under actual use conditions. Therefore, in these tests, variations in the temperature and rate of flow of the flue gas occurred during both on- and off-periods of the oil burner.

From the data of the tests conducted at the National Bureau of Standards and Battelle Memorial Institute, chimney efficiencies were computed and plotted in Fig. 10 as a function of the average temperature of the chimney gases observed at the lower temperature measuring station, which corresponds to the basement ceiling level in a residence.

[1] "Observed Performance of Some Experimental Chimneys," by R. S. Dill, P. R. Achenbach, and J. T. Duck, A.S.H.V.E. Transactions, Vol. 48, p. 351.

[2] Data taken from an unpublished progress report to Bituminous Coal Research, Inc., on "The Performance of Residential Chimneys," by R. B. Engdahl, P. C. Vyff, and F. B. Terrill, May 13, 1946.

Superimposed on this plot is the chimney efficiency which was obtained in the Research Home for an average temperature of the chimney gases at the basement ceiling level of 208 F, corresponding to an indoor-outdoor temperature difference of 34 F (see Fig. 9). The results of the three investigations are in close agreement even though there were differences in gas flow rates, cross-sectional areas, total heights, and methods of operation of the various chimneys.

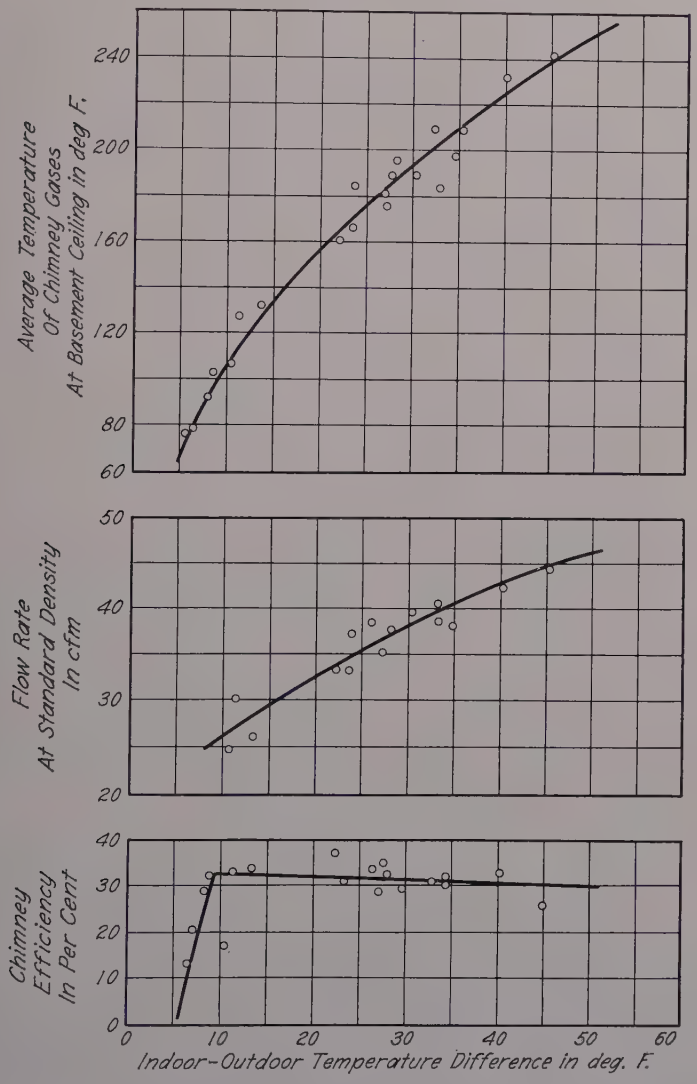

Fig. 9. Performance of Inside Chimney in I=B=R Research Home

Laboratory	Nominal Height Of Chimney ft.	Height Between Temperature Stations ft.	Method of Operation	Rate of Gas Flow In Chimney cfm. (std)
□ - Bur. Stds.	25	15	Continuous	67.5
○ - Bur. Stds.	30	15	Continuous	67.5
● - Bur. Stds.	35	15	Continuous	67.5
△ - Battelle	13	11.5	Continuous	40
▲ - Univ. of Ill.	35	17	Intermittent	45 on, 38 off

Laboratory	Inside Dimensions Of Chimney Inches	Chimney Location	Chimney Construction	Fuel
Bur. Stds.	$6\frac{1}{2} \times 11$	Outside	Liner, One Course Brick.	Gas
Batelle	$6\frac{3}{4} \times 6\frac{3}{4}$	Inside	Liner, One Course Brick.	Electricity
Univ. of Ill.	$6\frac{1}{2} \times 11$	Inside	Liner, One Course Brick, Air Space, Lath & Plaster.	Oil

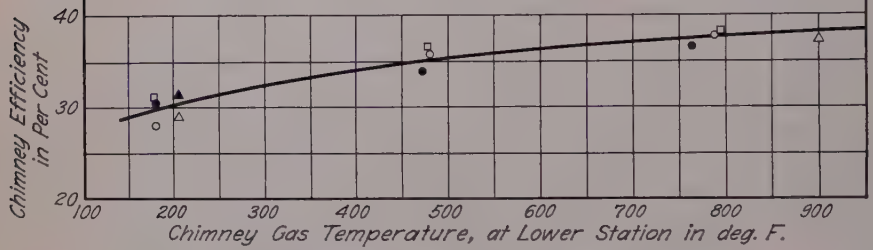

Fig. 10. Chimney Efficiencies Obtained from Three Investigations

The rates of gas flow in the chimney during the tests represented in Fig. 10 are representative of the flow rates required for the combustion of 1–1.5 gal of oil per hr with a CO_2 content in the products of combustion of 8 percent. A combustion rate of 1.5 gal of oil per hr is adequate to provide heat for a house having a calculated heat loss of about 150,000 Btu per hr. Some tests at the National Bureau of Standards were made of other flow rates. These seemed to indicate that the chimney heat transfer efficiency increased slightly as the gas flow rate was decreased below 67.5 cfh, but there were insufficient data to definitely establish the magnitude of the change.

In residential operation, the average temperature of the chimney gases will normally approximate 200 F, and should not exceed 500 F. It should be remembered that these are not maximum temperatures but include both on-period and off-period operation and that, furthermore, they are affected by the entrance of basement air through the draft regulators. Therefore it would appear that a chimney efficiency of 30–35 percent could be expected for an inside masonry chimney having a length of travel through the heated portion of the house of approximately 15 ft.

19. Heat Utilization

The amount of fuel required to offset the heat loss of the house is affected by the heat supplied to the house from the inside chimney. In addition, the heat from the chimney is not necessarily supplied to all rooms of the house in proportion to the heat loss of those rooms. Therefore, the heat supplied by the chimney affects both the utilization of fuel by the house and the distribution of heat within the house.

It may be assumed that the heat utilized by the house is the total heat available in the fuel burned minus the heat available in the chimney gases at the upper boundary of heated space. This is equivalent to the heat supplied to the house from the boiler and smoke pipe plus the heat supplied from the inside chimney; it may be expressed as

$$H_L = H_f E_u + H_f (1 - E_u) E_c \tag{23}$$

or

$$H_L = H_f [E_u + (1 - E_u) E_c] \tag{24}$$

in which

H_L = total heat utilized by the house, Btu per hr
H_f = total heat available in the fuel burned, Btu per hr
E_u = combined boiler and smoke pipe efficiency — that is, the available heat in the fuel minus the available heat in the chimney gases at the basement ceiling level divided by the available heat in the fuel burned
E_c = chimney efficiency, expressed in decimal form

The heat supplied to the house from the chimney gases is equal to the available heat in the chimney gases at the basement ceiling level multiplied by the chimney efficiency in decimal form and may be expressed as a ratio to the heat utilized by the house as

$$Q_c = \frac{H_f (1 - E_u) E_c}{H_f [E_u + (1 - E_u) E_c]} \tag{25}$$

or

$$Q_c = \frac{(1 - E_u) E_c}{E_u + (1 - E_u) E_c} \tag{26}$$

in which

Q_c = the heat obtained by the house from the chimney gases divided by the heat utilized by the house
E_u, E_c = the same as in Eq. 24

Equation 26 indicates that for any given value of chimney efficiency there is a direct relationship between the heat obtained by the house from the chimney divided by the heat utilized by the house, Q_c, and the combined efficiency of the boiler and smoke pipe, E_u. This relationship is shown in Fig. 11b for chimney efficiencies of both 30 and 35 percent.

Over-all house efficiency has been defined as the heat utilized by the house expressed as a percentage of the total heat available in the fuel burned. Hence, it is a measure of the heat in the fuel burned which is utilized by the house to offset heat losses. A discussion of the factors affecting over-all house efficiency is included in Appendix A.

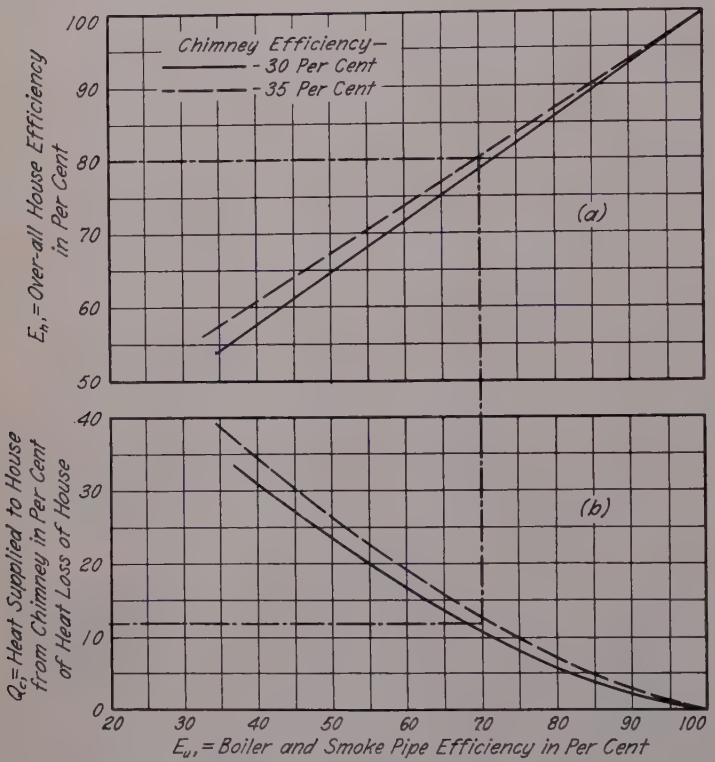
Chimney Efficiency—
30 Per Cent
35 Per Cent
E_h, = Over-all House Efficiency in Per Cent
(a)
(b)
Q_c = Heat Supplied to House from Chimney in Per Cent of Heat Loss of House
E_u, = Boiler and Smoke Pipe Efficiency in Per Cent

Fig. 11. Relationship Between Heat Obtained from Chimney and Operating Efficiencies

The following equation is an expression for over-all house efficiency:

$$E_h = \frac{H_L}{H_f} \tag{27}$$

By substituting the equivalent of H_L from Eq. 24, Eq. 27 becomes:

$$E_h = E_u + (1 - E_u)\, E_c \tag{28}$$

in which

E_h = the over-all house efficiency, expressed in decimal form
E_u, E_c = the same as in Eq. 24

For any given chimney efficiency, then, there is a direct relation between the over-all house efficiency, E_h, and the combined efficiency of boiler and smoke pipe, E_u. This relationship is shown in Fig. 11a for chimney efficiencies of both 30 and 35 percent, representative of the chimney efficiencies obtained with an inside masonry chimney in a two-story house.

When the chimney efficiency and either the over-all house efficiency or the combined efficiency of the boiler and smoke pipe are known, Fig. 11 may be used to determine the heat supplied to the house by the chimney as a percentage of the total heat utilized by the house, Q_c. Thus Q_c is independent of the type of construction of the house, the type of fuel burned, and the indoor-outdoor temperature difference.

As discussed in Section 18, the range of chimney efficiencies for an inside masonry chimney in a two-story house will normally be between the values of 30 and 35 percent. Results of heating research[1] have shown that over-all house efficiencies are generally 80 percent or less. Assuming an over-all house efficiency of 80 percent and a chimney efficiency of 33 percent, Fig. 11 shows that the combined efficiency of the boiler and smoke pipe is 70 percent and the heat supplied to the house by the chimney in percent of the total heat utilized by the house, Q_c, is 12 percent. For a two-story house, this averages 1.5 percent of the total heat utilized by the house for each side of the chimney exposed to a room. At design outdoor temperatures, the total heat utilized by the house is assumed to be equal to the calculated heat loss of the house. Therefore, to maintain uniform temperatures in the various rooms, the heat to be supplied by the installed radiation in a room should be reduced by an amount equal to 1.5 percent of the calculated heat loss of the *house* for each side of the chimney exposed to that room. For example, in a residence with a calculated heat loss of 100,000 Btu per hr, the reduction of installed radiation in a room to which two sides of the chimney are exposed would be equal to 3000 Btu per hr.

It is common practice to omit the heat losses of the basement from the calculated heat losses of the house, since the heat supplied from the boiler jacket and smoke pipe is normally sufficient to offset the basement losses. If the basement heat losses are omitted from the calculated heat losses of the house, the reduction of installed radiation in a room by an amount equal to 1.5 percent of the calculated heat losses of the house for each side of the chimney exposed to that room may be used with safety, as this allowance is somewhat less than that indicated by the test data reported in this bulletin.

[1] Univ. of Ill. Eng. Exp. Sta. Buls. 318, pp. 39–44, and 349, pp. 57–62.

If the combined efficiency of the boiler and smoke pipe decreases below 70 percent, the heat obtained from the chimney in percent of the heat loss of the house will increase, so that the preceding allowance of 1.5 percent is on the safe side. For example, at a combined efficiency of 60 percent, Fig. 11 shows that the heat obtained from the chimney will be about 18 percent of the heat loss of the house instead of the 12 percent obtained with a 70 percent combined efficiency.

The rate of heat transfer from the chimney to the first story of the house is greater than that to the second story, due to the greater difference between the temperatures of the chimney gas and the room air. Therefore, a reduction of installed radiation in a room by an amount equal to 1.5 percent of the calculated heat loss of the house for each side of the chimney exposed to that room may be used for one story houses as well as for two story houses.

VII. SUMMARY

The heat supplied to the house from the chimney was calculated by two methods: (1) from the observed flue gas temperatures and rates of flow, (2) from the observed plaster surface and room air temperatures. There was fair agreement in the quantity of useful heat obtained from the chimney as determined by these two independent methods of calculation.

When the I = B = R Research Home was being heated by a forced-circulation, hot-water system using an oil-fired boiler vented to the inside chimney, the heat supplied to the house from the chimney amounted to about 15 percent of the total heat loss of the house for normal winter temperature.

The heat supplied to the house from the chimney in average winter weather amounted to about 31 percent of the total heat available in the chimney gases at the basement ceiling level. That is, the chimney efficiency equalled 31 percent. This value was substantiated by the results of chimney studies made at Battelle Memorial Institute and the National Bureau of Standards.

The heat supplied to the house from the chimney expressed in percent of the total heat loss of the house is a function of the combined efficiency of the boiler and smoke pipe, and the length of chimney exposed to the heated space. It is not dependent upon the type of construction of the house, the type of fuel burned, or the indoor-outdoor temperature difference.

With a combined efficiency of the boiler and smoke pipe of 70 percent and a chimney efficiency of 33 percent the heat supplied to a two story house by an inside chimney would be about 12 percent of the heat loss of the house. At a combined efficiency of 60 percent, the heat obtained from the chimney would be about 18 percent of the total heat loss of the house. Since most of this heat would be lost to the outdoors if an outside chimney were used, it becomes apparent that use of an inside chimney results in increased economy of operation.

The heat obtained by the house from an inside chimney is of sufficient magnitude that it can cause an unequal distribution of heat in the house if an allowance is not made for the chimney heat supplied

to the rooms through which the chimney passes. It is suggested that in designing a heating system, the heat to be supplied by the installed radiation in a room should be reduced by an amount equal to 1.5 percent of the calculated heat loss of the *house* for each side of the chimney exposed to that room. This correction is based on a combined boiler and smoke pipe efficiency of 70 percent. The installed radiation thus selected should be adequate for either a one story or a two story house.

APPENDIX A: HEAT UTILIZATION AND OVER-ALL HOUSE EFFICIENCY

Heat utilization and over-all house efficiency are closely related to the heat supplied to the house from the chimney. In a previous bulletin[1] it was pointed out that when a central heating system is used in connection with an inside chimney, as was done in the case of the Research Home, the only part of the total heat input to the house that is not actually utilized in offsetting heat losses is the heat carried away by the chimney gases as measured at the level of the upper boundary of the heated space. This boundary usually is at the attic floor level. The over-all house efficiency is an index of the effectiveness of heat utilization, and serves as a convenient basis in making comparisons between different heating installations.

In the same bulletin a comparison was also made of the over-all house efficiency obtained with two methods of operating a hot-water heating system. It was pointed out that different methods of operation resulted in different house efficiencies. However, the discussion contained very little explanation of the causes of these differences. Since the writing of Bulletin 349, additional data have been obtained which warrant a discussion of the relationship between average boiler water temperature and over-all house efficiency. During the course of the testing program in the I = B = R Research Home a number of different heating systems and methods of operation have been employed. As shown in Fig. 12, the average temperatures of the water at the top of the boiler varied considerably for these methods of operation. In Fig. 13 the over-all house efficiency obtained for these same operating conditions is shown. It may be observed from a study of Figs. 12 and 13 that the method of operation which provides a lower temperature of boiler water for a given indoor-outdoor temperature difference results in a higher over-all house efficiency.

To demonstrate further the relationship of boiler water temperature to over-all house efficiency, the curves in Fig. 14 were constructed by plotting, for various indoor-outdoor temperature differences, the over-all house efficiency and the corresponding boiler water temperature as

[1] "Performance of a Hot-Water Heating System in the I=B=R Research Home at the University of Illinois," Univ. of Ill. Eng. Exp. Sta. Bul. 349, pp. 57–62. 1944.

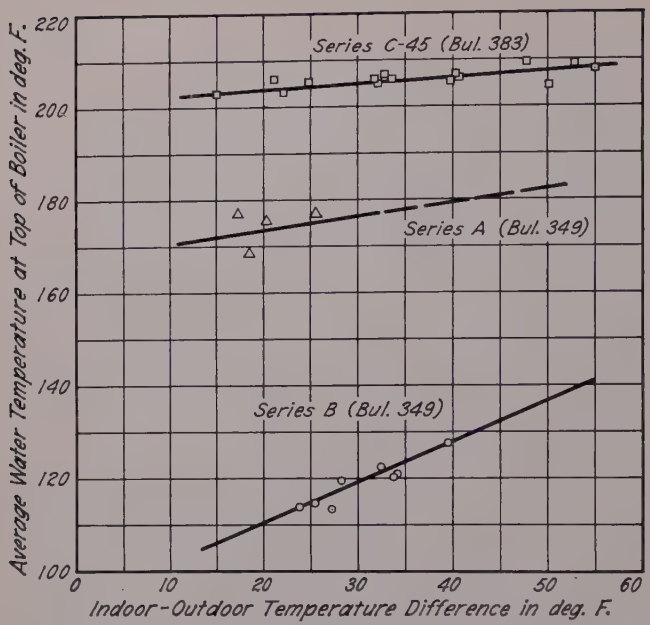

Fig. 12. Temperature of Water at Top of Boiler for Three Operating Conditions

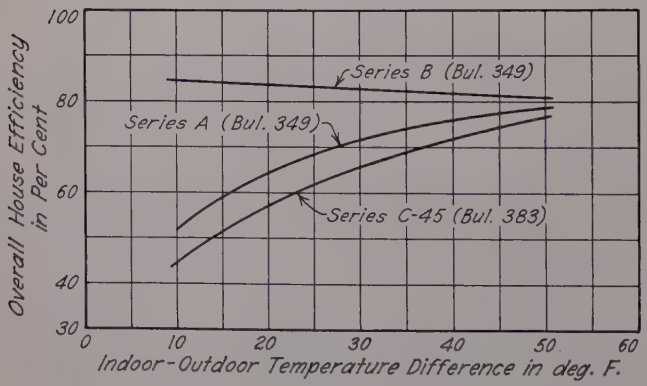

Fig. 13. Over-all House Efficiency, Three Operating Conditions

read from the appropriate curves in Figs. 12 and 13. For any indoor-outdoor temperature difference the relationship between the over-all house efficiency and the boiler water temperature is approximately linear. It should be noted that the slope of the curves increases with decreasing indoor-outdoor temperature differences. The family of curves demonstrates that the average temperature of the water in the boiler is not the only factor affecting the chimney loss, and therefore over-all

house efficiency. As the indoor-outdoor temperature difference increases, the effect of the average temperature of the water in the boiler on over-all house efficiency is decreased. This result is logical, since changes in the boiler water temperature have a pronounced effect on the off-period losses and a relatively small effect on the on-period losses, and the total off-period time increases with decreasing indoor-outdoor

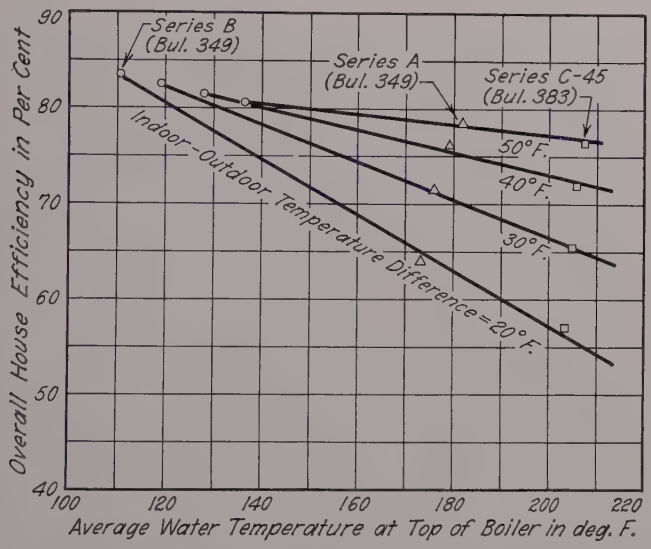

Fig. 14. Relationship Between Boiler Water Temperature and Over-all House Efficiency

temperature difference. Therefore the total time of burner operation is also a factor affecting house efficiency. While other factors also may be involved, it can be concluded that for a conventional steam or hot-water system operating in a given house, the over-all house efficiency is decreased as the boiler water temperature is increased, provided that there is little or no change in the total time per day that the burner is in operation. Moreover, as the actual operating time of the burner per day is decreased, the effect of water temperature on over-all house efficiency becomes more pronounced.

APPENDIX B: APPLICATION OF PROPOSED DESIGN PROCEDURE TO RESEARCH HOME

Data on the I = B = R Research Home are used here to illustrate the use of the procedure for the selection of radiation suggested in Section 19. Column (3) of Table 2 gives the total calculated heat loss of each room of the I = B = R Research Home at the design indoor-outdoor temperature difference of 80 F. Conventional practice in the design of a steam or hot-water heating system is to provide sufficient radiation in each room to offset this calculated design heat loss. Column (2) indicates the number of sides of the inside chimney which are exposed to the different rooms. Column (4) is the allowance for heat obtained from the chimney (taken as 1.5 percent of the calculated heat loss of the house for each side of the chimney exposed to the room), and column (5) represents the net heat to be provided by radiation after making allowances for the heat obtained from the chimney.

Using the conventional procedure the radiation would be selected in accordance with the values in column (3) of Table 2. By the procedure suggested in Section 19 the radiation would be selected on the basis of the values in column (5). Column (6) shows that in the Research Home the heat obtained from the inside chimney was sufficient to take care of from 11 to 30 percent of the normal heat requirements of the rooms to which the sides of the chimney were exposed.

In the description of the first heating system used in the Research Home, as given in Station Bulletin 349, it was stated that the amount of radiation installed in each room was just sufficient to offset the calculated heat loss of the room (column 3, Table 2). However, to obtain proper balance of room temperatures it was found necessary to reduce the radiation in the dining room and southwest bedroom by 35 and 25 percent respectively, whereas radiation in the living room was increased by about 9 percent.

In the southwest bedroom the reduction made in the amount of installed radiation corresponded very closely to the reduction indicated by the design procedure suggested in this bulletin. In the dining room the actual reduction was even greater than that indicated by the estimated chimney allowance. The boiler was located in the basement

directly under the dining room, and temperatures taken on either side of the dining room floor indicated that additional heat was supplied to this room through the floor.

Only in the living room was the actual change in radiation contrary to that indicated by the proposed procedure. Observations in the Research Home have indicated that the radiation installed in the vestibule

Table 2

Data on I=B=R Research Home Illustrating Use of Suggested Radiation Selection Procedure

Room	No. of Sides of Chimney Exposed to Room	Calculated Heat Loss, Btu per Hr	Heat Obtained from Chimeny, Btu per Hr	Net Heat to Be Supplied by Radiation, Btu per Hr	Reduction in Radiation Required, percent
(1)	(2)	(3)	(4)	(5)	(6)
Liv. Rm.	1	5749	650	5099	11.3
Din. Rm.	2	8742	1300	7442	14.9
Kitchen	1	3199	650	2549	20.3
Lavatory		1484		1484	
Vestibule		4848		4848	
N.E. Bed Rm.		4393		4393	
N.W. Bed Rm.	1	4944	650	4294	13.1
S.W. Bed Rm.	2	5250	1300	3950	24.8
Bath		2606		2606	
Stair	1	2155	650	1505	30.2
Total		43,370	5,200	38,170	12

was not adequate to keep the vestibule as warm as the remainder of the house. As a result cool air circulated through the open doorway from the vestibule into the living room, increasing the heat requirements of the latter. Had sufficient radiation been installed in the vestibule it is unlikely that additional radiation would have been required in the living room.

Actual performance therefore indicated that conventional procedures for the selection of radiation have resulted in too much radiation in those rooms of the Research Home to which two sides of the chimney were exposed. Furthermore, had the procedure suggested in Section 19 been used the room temperature balance would have been improved in every room with the possible exception of the living room, in which the unbalanced condition resulted largely from lack of sufficient radiation in the adjoining vestibule, rather than from heat obtained from the chimney.

Table 3
Daily Heat Supplied to House from Chimney Gases, Using Flue Gas Temperature Method

Date	Δt	N	ϕ_2		t_c		t_b		W_d		t_m	t_p	H_d*		H_c*	H*
			on-period	off-period	on-period	off-period	on-period	off-period	on-period	off-period			on-period*	off-period*		
2/ 9/42	45.2	25	14.1	43.5	241	178	377	198	271	178	274	418	52.0	15.5	3.2	70.7
2/18/42	63.7	33	15.0	28.6	255	201	...	...	304	218	291	...	....	....	...	....
3/ 3/42	40.2	25	11.7	45.9	225	163	372	198	274	179	256	412	47.1	28.8	3.0	78.5
3/ 4/42	33.2	19	11.3	64.5	218	150	367	183	266	170	249	406	33.9	28.4	2.3	64.6
3/ 5/42	33.2	16	12.2	77.5	216	136	370	156	264	161	246	411	31.6	16.0	2.2	49.8
3/10/42	26.4	14	12.4	90.8	209	137	361	156	265	162	238	401	28.2	23.2	1.9	53.3
3/12/42	34.7	19	10.7	65.0	210	144	361	170	263	157	240	400	32.0	20.4	2.2	54.6
3/14/42	34.9	20	11.3	60.7	214	151	366	178	262	156	244	406	36.1	20.8	2.5	59.4
3/19/42	27.0	15	10.5	85.5	206	137	355	153	260	147	235	394	24.3	12.2	1.7	38.2
3/23/42	23.6	13	11.1	99.7	202	128	358	145	256	140	230	398	23.1	12.5	1.6	37.2
3/26/42	27.8	18	10.3	69.6	199	136	359	165	262	158	227	398	30.9	22.6	2.2	55.7
4/ 3/42	22.1	13	9.8	101.0	200	120	359	141	254	142	228	398	20.6	15.7	1.5	37.8
4/12/42	28.0	18	10.4	69.6	210	142	364	170	260	152	239	405	30.0	21.3	2.1	53.4
4/13/42	23.7	15	11.2	84.7	208	115	364	161	262	156	237	404	27.3	36.5	1.9	65.7
4/14/42	11.4	7	10.4	195.4	190	107	343	115	255	131	217	381	11.4	9.8	0.8	22.0
4/19/42	30.0	17	12.5	72.4	212	140	361	159	266	163	241	401	33.6	15.5	2.3	51.4
4/22/42	....	7	8.4	197.3	182	102	328	112	248	114	207	364	8.5	5.9	...	....
4/23/42	10.4	5	8.4	279.7	183	102	326	99	245	91	209	362	5.9	−1.1	0.4	5.2
4/24/42	8.3	3	9.0	471.0	178	88	327	88	246	79	203	363	4.0	0.0	0.3	4.3
4/25/42	8.7	5	8.0	280.2	175	90	316	96	246	97	199	350	5.6	3.1	0.4	9.1
4/26/42	13.3	8	9.6	170.4	184	109	328	121	244	112	209	364	10.8	7.0	0.8	18.6
4/27/42	6.3	2	9.0	711.0	176	85	313	83	440	84	201	347	2.4	−1.0	0.2	1.6
4/28/42	6.7	3	9.0	471.0	173	86	314	84	241	82	197	349	3.7	−0.8	0.3	3.2

* In 1000 Btu.

Δt = indoor-outdoor temperature difference, F
N = number of burner operating cycles per day
ϕ_2 = average duration of on-period or off-period, min
t_c = average temperature of chimney gas at the level of the attic floor, F
t_b = average temperature of chimney gas at the level of the basement ceiling, F
W_d = average rate of flow of dry chimney gas, lb per hr
t_m = temperature of chimney gas at the level of the attic floor at end of on-periods, F
t_p = temperature of chimney gas at the level of the basement ceiling at end of on-period, F
H_d = heat supplied to house from dry chimney gas, Btu
H_c = heat supplied to house from water-vapor formed by combustion of hydrogen in the fuel, Btu
H = total heat supplied to house from chimney gas, Btu

Table 4

Daily Heat Supplied to House from Chimney Gases, Using Plaster Surface Temperature Method

Date	(Δt)	t_1	t_3	(t_1-t_3)	t_2	t_4	(t_2-t_4)	h_1	h_2	H
2/ 9/42	45.2	90.5	73.6	16.9	90.1	74.9	15.2	54 250	43 900	98 150
2/18/42	63.7	94.9	74.5	20.4	92.9	75.0	17.9	65 500	51 750	117 250
3/ 3/42	40.2	88.0	74.1	13.9	88.1	75.4	12.7	44 600	36 700	81 300
3/ 4/42	33.2	86.7	73.7	13.0	87.5	75.3	12.2	41 700	35 250	76 950
3/ 5/42	33.2	85.7	74.3	11.4	86.0	75.6	10.4	36 600	30 020	66 620
3/10/42	26.4	84.7	73.5	11.2	86.2	75.4	10.8	35 950	31 200	67 150
3/12/42	34.7	84.7	73.6	11.1	85.7	75.3	10.4	35 650	30 020	65 670
3/14/42	34.9	86.0	73.2	12.8	86.6	74.8	11.8	41 050	34 100	75 150
3/19/42	27.0	84.9	73.9	11.0	85.5	75.4	10.1	35 300	29 200	64 500
3/23/42	23.6	85.9	74.8	11.1	85.9	75.1	10.8	35 650	31 200	66 850
3/26/42	21.8	82.4	73.2	9.2	81.2	74.2	7.0	28 250	20 220	48 470
4/ 3/42	22.1	81.7	73.5	8.2	83.6	76.7	6.9	26 350	19 650	46 000
4/12/42	28.0	85.8	73.3	12.5	87.1	77.3	9.8	40 100	28 350	68 450
4/13/42	23.7	84.8	72.9	11.9	86.3	76.3	10.0	38 200	28 880	67 080
4/14/42	11.0	81.2	73.5	7.7	82.9	77.1	5.8	24 700	16 760	41 460
4/19/42	30.0	85.3	73.8	11.5	88.8	77.5	11.3	36 900	32 650	69 550
4/22/42		81.3	74.4	6.9	83.0	77.7	5.3	22 150	15 320	37 470
4/23/42	10.4	79.2	74.3	4.9	81.6	78.2	3.4	15 720	9 830	25 550
4/24/42	8.3	78.5	75.0	3.5	80.6	78.3	2.3	11 250	6 650	17 900
4/25/42	8.7	77.6	73.9	3.7	79.0	76.3	2.7	11 900	7 800	19 700
4/26/42	13.3	78.2	72.9	5.3	79.0	75.7	3.3	17 020	9 540	26 560
4/27/42	6.3	77.6	74.1	3.5	80.2	77.6	2.6	11 250	7 510	18 760
4/28/42	6.7	76.5	74.2	2.3	79.2	77.7	1.5	7 380	4 330	11 710

H = total heat supplied to house from chimney gases = $(h_1 + h_2)$
h_1 = heat supplied to first story rooms from chimney gases, Btu = $C_1 (t_1 - t_3)$
h_2 = heat supplied to second story rooms from chimney gases, Btu = $C_2 (t_2 - t_4)$
C_1 = a constant = $\Phi a_1 f_i = 3208$
C_2 = a constant = $\Phi a_2 f_i = 2887$
a_1 = area of plaster wall exposed to rooms and enclosing chimney on first story, sq ft
a_2 = area of plaster wall exposed to rooms and enclosing chimney on second story, sq ft
t_1 = average surface temperature of a_1, F
t_2 = average surface temperature of a_2, F
t_3 = average room air temperature of first story, F
t_4 = average room air temperature of second story, F
Φ = time, hr
f_i = surface conductance, Btu per hr (sq ft) (F) = 1.65
Δt = indoor-outdoor temperature difference, F

I. INTRODUCTION

During the past few years, in this country and abroad, considerable work has been done in the theoretical and experimental study of stress and strength conditions arising when two cylinders are rolled together under pressure. This increased interest has been a result of the higher demands placed upon machine members which are constrained to work under similar conditions. Prime examples of such machine elements are gears and roller bearings.

Up to the present time the methods for determining the stress distribution and strength conditions in the contact zone of machine parts have been based, in general, on static rather than dynamic loading conditions. It is apparent that in modern high-speed machines the results based on such an approximation only approach actual values.

1. Purpose and Scope of Investigation

The purpose of the following investigation was twofold:

(1) To extend knowledge of the stress conditions in the contact zone of two compressed cylinders when rolled together with their axes parallel, by studying (a) the stresses outside the plane of symmetry and (b) their variation during the loading cycle by rolling of the cylinders.

(2) To investigate the strength condition of materials so studied and to suggest a method for its calculation in machine parts working under similar conditions.

The purposes mentioned above were carried out as follows: A review was made of the literature on character of failure of machine members as well as on experimental and theoretical investigations of the contact problem. For determination of stress variation in the contact zone of two rolling cylinders two methods were suggested — one in which the influence lines of stresses caused by the concentrated force are used, and the other an analytical method.

The first method does not require complicated mathematical calculations and has the further advantage that the loading curve of any form can be investigated. But the results obtained by using this method are only approximate. It does give satisfactory results for points which are located sufficiently far from the contact surface.

The analytical method was used for determinating stress components which are used for strength calculation. This method is based on the Belayev's three-dimensional solution of the problem of two cylinders of infinite length pressed together. Using this solution, the author investigated the variation of normal and tangential stress components in the contact zone when the cylinders are rolling one upon the other. On the basis of these investigations, a number of diagrams were plotted representing the variation of the normal and tangential components for the points located at various distances from the contact surface. One of the significant results from these investigations was that the stress component τ_{xy} has a completely reversed range.

The data on the absolute values and range ratios of stress at various layers in the contact zone were used to develop an equation for expressing the dynamic criterion of failure for rolling cylinders, or members operating under similar conditions. This equation is based on the Huber-Mises energy hypothesis. A table and a diagram showing the relationship between the critical pressure on the contact surface and the mechanical properties of different steels were prepared from data obtained by using this equation. The table also shows the location of the critical layer in the contact zone and its dependence upon the mechanical properties of materials. It should be noted that the distance of the critical layer from the contact surface for the conditions of dynamic loading does not coincide with the location of the point where the maximum shearing stress exists. In the author's opinion, the results obtained give a basis for calculating the strength of machine members working under similar conditions of dynamic loading.

The investigation is limited to the case of two cylinders rolling together without sliding. The case of rolling with sliding is likewise of great interest. At present, however, the actual distribution of the tangential forces acting on the lubricated surfaces of cylinders rolling with relative sliding is not known. It seems probable that in this case the friction between dry, half-dry, and lubricated surfaces takes place simultaneously and that the tangential loading on the contact surface is not proportional to the normal loading at the corresponding points. In the author's opinion, a study of the actual distribution of the tangential loading on the surface for this case must be made before the problem of the stress distribution and strength condition can be solved.

2. Acknowledgments

This work is based partly upon previous investigations conducted by the author at the Institute of Applied Mechanics of Academy of Sciences

of the Ukrainian SSR, Kiev, before coming to the United States. World War II prevented completion of this work until the present time.

The author wishes to thank Professors N. A. Parker, head of the Department of Mechanical Engineering, and D. G. Ryan, who is in charge of the Machine Design Group, for the opportunity to complete this investigation as part of the research program of the Machine Design Group. The assistance of D. H. Offner, instructor in the Department of Mechanical Engineering, is acknowledged for his help in the initial presentation of the written material.

II. PREVIOUS DATA ON CHARACTER OF FAILURE OF VARIOUS MACHINE MEMBERS

3. Character of Fatigue Failure of Gear Teeth and of Ball and Roller Bearings

Gear teeth failures caused by repeated contact stresses usually occur on the surface of the tooth along the intersection of the tooth face and the pitch cylinder. The failure appears as a crumbling of fine metal particles, causing the surface to be pitted. Such a condition results in severe wear.

A similar phenomenon can be observed in ball and roller bearings, where the fatigue failure causes the surface metal of the bearing races to come off in the form of thin flakes. The surface soon becomes rough and the bearing noisy. Failure progresses rapidly and the member must be replaced soon after flaking begins. According to Turkish*, the phenomena of pitting and flaking can likewise be observed on the working faces of cams and tappets of valve gears of internal combusion engines. The flaking phenomenon also develops whenever excessive variable contact stresses are present in machine parts operating under similar conditions, such as rails or on the wheels of cranes.

Various theories have been proposed to explain this phenomenon of pitting and flaking. At present it is fairly well established that pitting and flaking are caused by a great many cycles of repeated stresses which cause a fatigue failure of the metal in a relatively thin layer near the working surface of the members.

4. Experimental Investigations with Roller Machines

In the past fifteen years several experimental investigations have been conducted to determine the factors that cause pitting and flaking. The experiments made by S. Way†, T. Nishihara and T. Kobayashi‡, and A. Meldahl¶ are especially significant.

The experiments were made with roller machines so constructed that two metal cylinders could roll while being pressed together with any desired force. In Way's experiments the cylinders were made to roll

* M. C. Turkish, "Valve Gear Design," Detroit, 1946.
† S. Way, Journ. of Applied Mechanics, Vol. 2, Nos. 2 and 3, 1935; Machine Design, March 1939; Journ. of Applied Mechanics, Vol. 7, No. 4, 1940; Trans. A.S.M.E., Vol. 57, 1935.
‡ T. Nishihara and T. Kobayashi, Trans. Soc. Mech. Engrs. Japan, Vol. 3, 1937. (Japanese)
¶ A. Meldahl, Engineering, Vol. 148, July 21, 1939.

against each other without sliding. However, in the experiments of Nishihara and Kobayashi, and Meldahl the relative surface speeds of two cylinders were adjustable, permitting sliding to occur.

The results of these investigations showed clearly that pitting is caused by fatigue failure of the surface layer of metal and that it depended upon the magnitude and number of repeated load applications. The relationship between the number of stress applications and the pressure causing pitting on the surface was found to be very similar to the ordinary fatigue curves.

These experiments indicated also how the critical pressure depended on the relative sliding speed. It was found that the "surface endurance limit" decreased slightly when the relative sliding speed was increased from 0 to 20 percent, but increased again as the relative sliding speed went above 20 percent. This result was probably due to increased friction which caused the surface layer to wear off before fatigue failure could take place.

III. DISTRIBUTION OF STRESSES IN ZONE OF CONTACT

5. H. Hertz' Investigation

The general method for determining the distribution of stresses in the zone of contact of two elastic bodies was indicated by H. Hertz* in 1881. Of most interest are the following basic types of contact between two bodies: (1) bodies initially having point contact before the deformation, such as two spheres, a sphere and a plane, or a sphere and a cylinder, and (2) bodies having straight line contact before deformation, such as two cylinders with parallel axes or a cylinder and a plane. Practical illustrations of the first type of contact are ball bearings and their supports and wheels rolling on convex rails; illustrations of the second type are roller bearings and gears.

Hertz derived mathematical expressions for the distribution of pressure on the contact area of bodies having an initial point contact. He also was able to determine the limiting size of the axes of the elliptical contact area and the relative displacements of the bodies. For circular areas of contact, Hertz was able to determine the stress in the center of the area. For bodies having initial line contact, he obtained expressions defining the width of the contact strip and the pressure distribution across this strip.

According to Hertz, the pressure distribution on the surface of two compressed bodies is defined by the expression (see Fig. 1)

$$p = p_{\max} \sqrt{1 - \frac{y^2}{b^2}} \tag{1}$$

where $p_{\max}$ = maximum pressure at center of contact area for the initial point contact and at the middle of strip for the initial line contact

y = the distance from the x-axis

b = semi-axis of elliptical contact area or one-half the width of contact strip

Figure 2 shows the pressure distribution across the surface of the contact strip of two cylinders. It also shows the position of the axes

* H. Hertz, Journ. Math., Vol. 92, 1881. See also H. Hertz' "Gesammelte Werke," Vol. 1. Leipzig, 1885.

in the coordinate system. The value of the maximum pressure on the middle of the contact strip is

$$p_{max} = \sqrt{\frac{1}{\pi(1-\mu^2)} \cdot \frac{P}{l} \cdot \frac{\frac{1}{R_1}+\frac{1}{R_2}}{\frac{1}{E_1}+\frac{1}{E_2}}} \tag{2}$$

where μ = Poisson's ratio for the two materials
P = force pressing the two cylinders together
E_1, E_2 = modulus of elasticity in compression for cylinders 1 and 2
R_1, R_2 = radii of the two cylinders
l = length of the cylinders

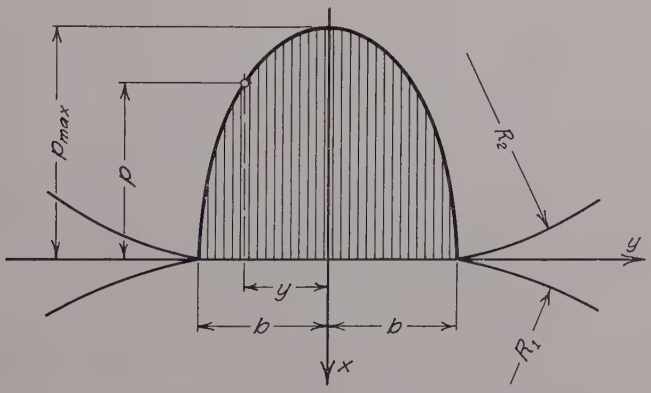

Fig. 1. Pressure Distribution on Contact Surface

The value of b for two cylinders with parallel axes can be obtained from the expression:

$$b = 2\sqrt{\frac{1-\mu^2}{\pi} \frac{P\left(\frac{1}{E_1}+\frac{1}{E_2}\right)}{l\left(\frac{1}{R_1}+\frac{1}{R_2}\right)}} \tag{3}$$

For steel, using $\mu = 0.3$ and $E_1 = E_2 = E$, the magnitude of one-half the width of the contact strip is:

$$b = 1.52\sqrt{\frac{P}{El} \frac{R_1 R_2}{R_1 + R_2}} \tag{4}$$

and the maximum pressure on the middle of the contact strip is:

$$p_{max} = 0.418 \sqrt{\frac{PE}{l}\left(\frac{1}{R_1} + \frac{1}{R_2}\right)} \tag{5}$$

In making this analysis Hertz used the following assumptions:

1. The bodies in contact are isotropic
2. The proportional limit of materials is not exceeded
3. The loading acts perpendicular to the surface
4. The dimensions of the compressed area are small when compared with the whole surface of the bodies pressed together
5. The radii of curvature of the contact areas are very large compared with the dimensions of these areas

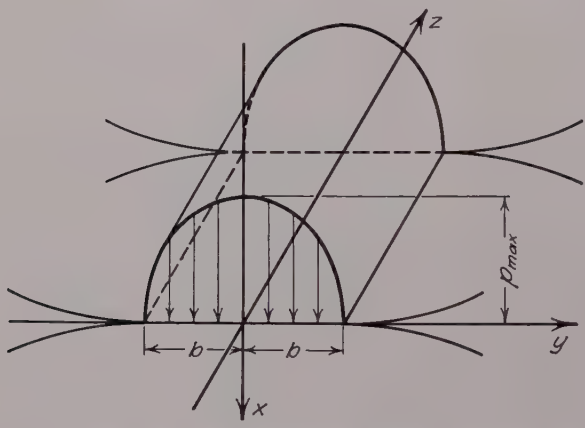

Fig. 2. Pressure Distribution Across the Strip of Contact Surface of Two Cylinders

6. Later Investigations of the Hertz Problem

Using the same assumptions listed above, later investigators extended Hertz' work. In 1924 Belayev* in Russia, and independently Thomas and Hoersch† in this country and Föppl‡ in Germany determined the law of distribution for the stress components along the x-axis in the plane of symmetry of the loading curve. Figure 3 shows the distribution of stress components σ_x, σ_y, and σ_z, and the stress $\tau_{45°}$ along the line of symmetry for two cylinders pressed together with parallel axes. The ordinate representing the distance of the points from the contact surface is given in terms of b. Except for the values of normal stress components, the diagram also represents the variation in value of $\tau_{45°}$. The stress $\tau_{45°}$ is the

* N. M. Belayev, Mag. Eng. Buildings and Applied Mech., St. Petersburg, 1924. (Russian)
† H. R. Thomas and V. A. Hoersch, "Stresses Due to the Pressure of one Elastic Solid upon Another," Univ. of Ill. Eng. Exp. Sta. Bul. No. 212, 1930.
‡ L. Föppl, Forschung auf d. Gebiete d. Ingenieurwesens, No. 5, 1936.

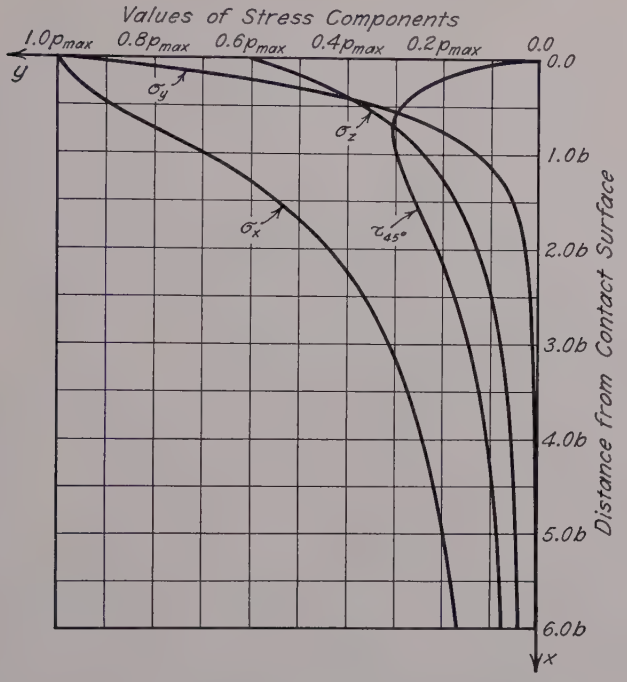

Fig. 3. Distribution of Stresses in Contact Zone Along Line of Symmetry

shearing stress on a plane which makes an angle of 45 deg with the y-axis. The value is

$$\tau_{45°} = \frac{\sigma_x - \sigma_y}{2} \tag{6}$$

at the plane of symmetry.

Belayev, Thomas and Hoersch, and Föppl all found that the maximum shearing stress in the zone of contact of two cylinders having parallel axes acts on a plane which bisects the angle formed by the y- and x-axes ($\varphi = 45°$). This stress is located at the point where $x \cong 0.78\ b$ from the contact surface. The value of the shearing stress τ_{xy} in the plane of symmetry is zero. According to Belayev, the value of maximum shearing stress when $\mu = 0.3$ is

$$\tau_{max} = 0.304 p_{max} = 0.304 \frac{2P}{l\pi b} = 0.304 \frac{2q_0}{\pi b}$$

where q_0 is the loading per unit length of cylinder.

The more recent works of Poritsky* and Liu† should also be mentioned. Poritsky expressed the equation for two-dimensional stresses and deflections of two cylindrical bodies in contact under normal and tangential reactions in terms of Airy's function. He has taken the tangential load

* H. Poritsky, Journal of Applied Mechanics, Vol. 17, No. 2, June 1950.
† C. K. Liu, Thesis for the degree of Doctor of Philosophy, University of Illinois, 1950.

as being proportional to the normal Hertz' load over the same area. He considered that the ratio between the tangential and normal load was equal to the constant coefficient of friction, 0.3.

Liu independently solved the same problem by the method of real variables both for cases of plane stress and plane strain. He pointed out that the stresses which appear in the region of contact caused by the presence of tangential forces deserve attention. He also assumed that the intensity of the tangential force at every point in the contact area is proportional to the normal force at the same point. His factor of proportionality is equal to $\frac{1}{3}$.

7. Factors of the Hertz Problem Not Considered

There are some indications that tensile stresses occur on the surface layer of compressed bodies at points which lie outside of, but very close to, the area of pressure contact. When two bodies are rolled together, the surface areas are stressed in tension and then in compression. For brittle materials it is possible that these tensile stresses, which occur near the border of the contact area, contribute to the fatigue failure of the surface. It seems possible that this phenomenon would be important in the case of two cylinders having a large difference between their radii. The condition could be especially critical on the surface of the larger cylinder because it would have a concave contact surface.

This phenomenon was not taken into account by Hertz' analysis and those expanding his work.

Lubrication is also a factor which can have some influence on the stress distribution on the contact zone, and which was not taken into account by Hertz' analysis. S. Way believed that initial cracks were formed very near the surface due to the repeated contact stresses. When these cracks progress to the surface, the oil is pressed into the openings, causing further cracking, and resulting in pitting as the metal is crumbled and torn from the surface. Way suggests that by using oil of high viscosity, the time at which pitting appears may be increased. However, the experiments of Nishihara and Kobayashi do not confirm this opinion. Apparently, the use of high viscosity lubricants decreases the duration of ball bearing life.

Very little reliable data are available regarding the manner in which the use of lubricants affects the fatigue failure of compressed bodies. The oil layer between the rolling cylinders also affects the pressure distribution on the surface of compressed bodies, and thus also changes the stress

conditions in the contact zone. The results of some investigations indicate that these changes in pressure distribution due to lubrication are relatively small and affect the stress very little. Figure 4 shows how Eichinger suggested that the pressure distribution may be effected by lubrication.

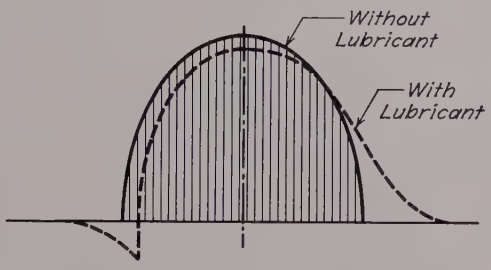

Fig. 4. Pressure Distribution With and Without Lubricant, According to Eichinger

8. Strength Calculation of Materials Based on Data Obtained from Stress Distribution Along the Plane of Symmetry

Several authors have suggested using the maximum shear stress for gear calculations. Among them are Schmitter*, Petrusyevich†, Dollezhal‡. Buckingham¶ and Wissman§ recommended using the maximum pressure on the contact area as an initial value in gear calculation. T. Barish** also used the maximum Hertz' pressure as a basic stress for calculations on ball bearings.

Since the maximum shearing stress in elastic bodies which are pressed together is directly proportional to the maximum pressure on the contact area, there is no difference of principle between the methods of determining the permissible stress as proposed by Schmitter and Petrusyevich or Buckingham, Wissman and Barish.

Eichinger†† suggested using the reduced stress σ_r for calculating the strength in the contact zone of two cylinders with parallel axes. This

* W. P. Schmitter, Machine Design, July 1934.

† Petrusyevich, The works of "Central Bureau Reducter Building Orgametall," Moscow, 1939. (Russian)

‡ V. Dollezhal, Techn. of Air Fleet, No. 5, May 1939. (Russian)

¶ E. Buckingham, Manual of Gears Design, Sect. No. 2, 1935; Manual of Gears Design, Sect. No. 3, 1937.

§ K. Wissman, Berechnung und Konstruktion von Zahnrädern für Kräne und ähnliche Maschinen, Dissertation, Duisburg, 1930.

** Thomas Barish, "A Theoretical Derivation of Ball Bearing Ratings," Paper No. 46-A-75 prepared by Engineering and Research Corporation, Riverdale, Maryland, for presentation at the annual ASME meeting of 1946 (Advance copy).

†† E. Eichinger, "Reibung und Verschliess," Stuttgart, 1938.

reduced stress σ_r should be compared to the mechanical properties of metal by direct pressure, for example to the compressive yield point σ_s.

The value of the reduced stress according to Eichinger (using the Mises-Hencky's hypothesis) may be found from the equation:

$$\sigma_r = \sqrt{\sigma_x^2 + \sigma_y^2 + \sigma_z^2 - \sigma_x\sigma_y - \sigma_y\sigma_z - \sigma_x\sigma_z} \qquad (7)$$

Figure 5, shows the variation in the value of σ_r along the axis of symmetry. On the axis of symmetry, the maximum value of σ_r is

$$(\sigma_r)_{\max} = 0.55\sigma_{ox}$$

where $\sigma_{ox} = p_{\max}$. The maximum reduced stress occurs at a point $x \cong \frac{2}{3}\, b$ from the contact surface.

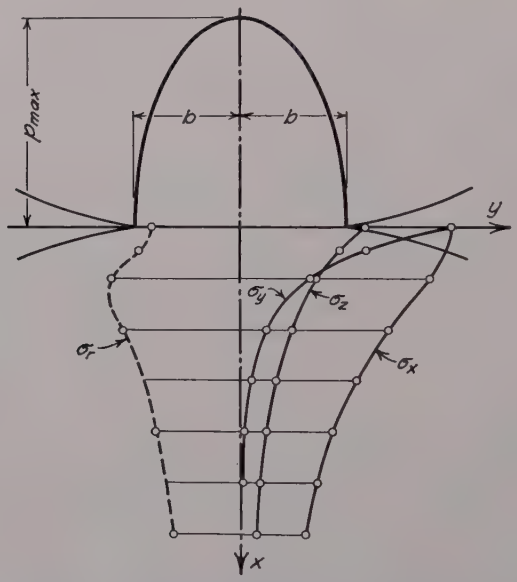

Fig. 5. Variation in Value of Reduced Stress Along Axis of Symmetry, According to Eichinger

On the surface at the middle of the contact strip

$$\sigma_r = 0.4p_{\max}$$

Mundt* and Treyer† used the reduced normal stresses at the middle of the contact area as the basis for calculations on ball and roller bearings.

* R. Mundt, Forschung auf d. Gebiete d. Ingenieurwesens, Bd. 3, 1932, S. 127.
† Treyer, The Theory and Calculation of Ball and Roller Bearings, 2d ed., Moscow, 1936. (Russian)

IV. ANALYSIS OF STRESS VARIATION IN CONTACT ZONE OF TWO COMPRESSED CYLINDERS ROLLING TOGETHER

The fatigue strength of materials subjected to repeated loading is known to depend not only on the maximum stress but also upon the manner in which the stresses vary during a loading cycle. It was the purpose of this investigation to determine this stress variation at every desired point in the contact zone of two rolling cylinders. Two methods of analysis were used in this investigation*.

9. Method of Influence Lines of Stresses

According to Flamant† the normal components of stress σ_x and σ_y and the shearing stress τ_{xy}, which occur in an elastic medium limited by a plane due to a normal force P concentrated at a point, can be determined as follows: (See Fig. 6a)

$$\left.\begin{aligned} \sigma_x &= -\frac{2P}{\pi H}\cos^4\theta \\ \sigma_y &= -\frac{2P}{\pi H}\sin^2\theta\cos^2\theta \\ \tau_{xy} &= -\frac{2P}{\pi H}\sin\theta\cos^3\theta \end{aligned}\right\} \tag{8}$$

These equations were derived by Flamant using the Boussinesq‡ three-dimensional solution. Defining φ as the angle between the y-axis and plane on which the stresses to be found are acting (see Fig. 6b), the equation for the normal and shearing stresses on this plane can be determined as follows:

$$\sigma = \sigma_x\cos^2\varphi + \sigma_y\sin^2\varphi + 2\tau_{xy}\sin\varphi\cos\varphi \tag{9}$$

$$\tau = \tau_{xy}(\cos^2\varphi - \sin^2\varphi) + (\sigma_y - \sigma_x)\sin\varphi\cos\varphi \tag{10}$$

* These methods are briefly discussed in the author's article, "About the Strength by Repeated Contact Stresses," Inst. of Mech. Knowledge, Academy of Sciences USSR, 1941. (Russian)

† Flamant, "Comptes rendus," Vol. 114. p. 1465, Paris, 1892.

‡ J. Boussinesq, "Application des potentiels à l'étude de l'équilibre et du mouvement des solides elastiques," Paris, 1885. See also S. Timoshenko, "Theory of Elasticity," New York, 1934.

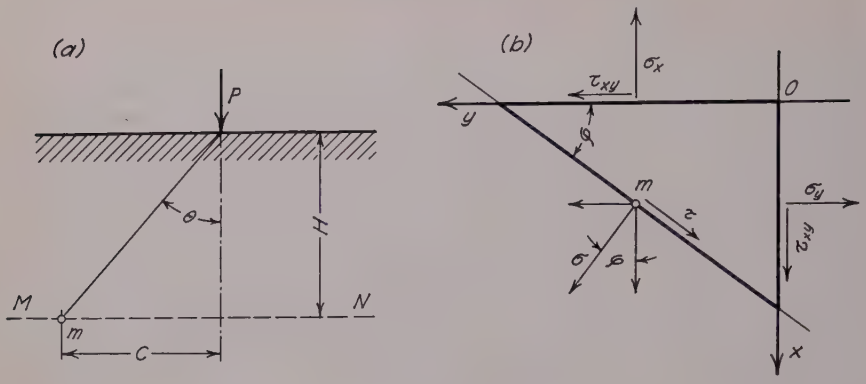

Fig. 6. Single Concentrated Force Acting Perpendicular to a Plane

By substituting Eqs. 8 into Eqs. 9 and 10, it is possible to find the values of σ and τ at any desired point in the stressed zone caused by the concentrated force P. In Fig. 7 values of stresses σ_x and τ_{xy} at a set of points a, b, c, ... n, located a distance H below the surface, have been plotted and connected by the smooth lines. These lines show how the stresses vary along the line p–q due to the concentrated load P. At the same time they can be considered as the influence lines for the stresses (in this case stresses σ_x and τ_{xy}), at the point B due to the concentrated force P.

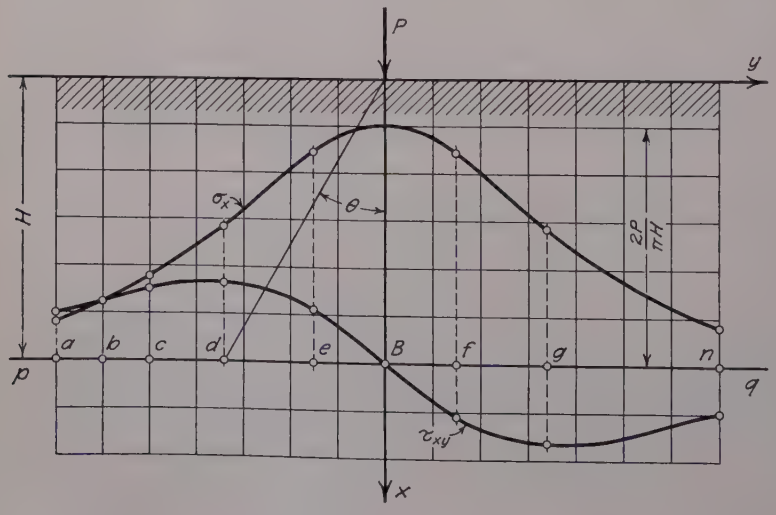

Fig. 7. Influence Lines of Stresses Due to a Single Concentrated Force

This method was applied to the stress analysis of two rolling cylinders as follows:

1. Referring to Fig. 8a, a curve showing the pressure distribution across the contact strip of a cylinder of unit length was constructed from the base line A–B. For the case of two cylinders with parallel axes, the curve is a semi-ellipse. This area was divided into a number of parts by vertical lines. Concentrated forces P_1, P_2, . . . P_n were assumed to be applied at the center of gravity of each area and their magnitudes were assumed equal to the areas they replaced.

2. Influence lines of the stresses were then constructed for the single concentrated force P_1 having an assumed magnitude of unity. In the example of Fig. 8, the stresses $\tau_{45°}$ and τ_{xy} are shown at the point where $x = 0.78\ b$. According to Belayev, the shearing stress $\tau_{45°}$ reaches its maximum value at this point. In Fig. 8b, curve 1 represents the influence line of stress $\tau_{45°}$ and curve 2 represents the influence line of stress τ_{xy} for the unit force, P_1.

3. Using the influence lines 1 and 2, the influence lines of stresses $\tau_{45°}$ and τ_{xy} for the whole system of forces P_1, P_2, . . . P_n can be constructed (Fig. 8c). These curves now show the variation $\tau_{45°}$ and τ_{xy} at the point lying in a layer where $x = 0.78\ b$, by moving the system of forces along the line A–B.

The results thus obtained are an approximate analysis of the stress variations existing in two rolling cylinders. The degree of accuracy can be

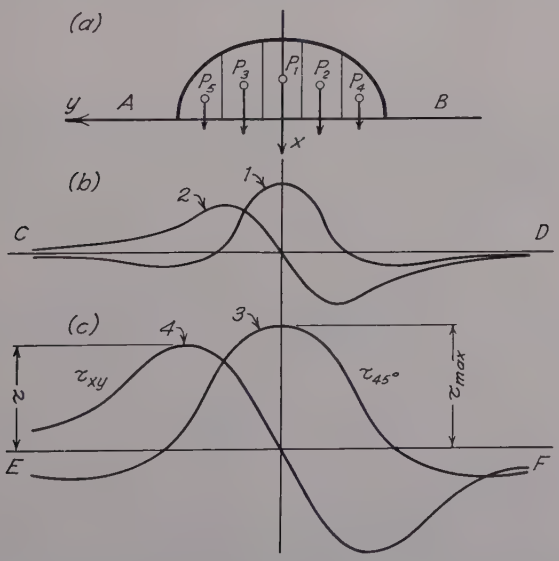

Fig. 8. Method Using Influence Lines of Stresses, Caused by a Series of Concentrated Forces

increased by dividing the loading into a greater number of parts and by increasing the distance H between the points and the surface of the body.

By comparing the different results it was found that when the area of the semi-ellipse was divided into seven parts, satisfactory values of stress were obtained at points about 0.5 b or farther from the surface.

10. Analytical Method of Analysis

The second method of analysis for determining the stress distribution during a loading cycle is entirely analytical. This analysis is based on work done by Belayev*. He found that the stresses on planes perpendicular to the coordinate axes can be calculated by the following equations expressed in elliptic coordinates:

$$\left.\begin{aligned}
\sigma_y &= -\frac{2q}{\pi b} e^{-\alpha} \sin\beta + \frac{2q}{\pi b} \sin\beta \sinh\alpha \left(1 - \frac{\sinh 2\alpha}{\cosh 2\alpha - \cos 2\beta}\right) \\
\sigma_x &= -\frac{2q}{\pi b} e^{-\alpha} \sin\beta - \frac{2q}{\pi b} \sin\beta \sinh\alpha \left(1 - \frac{\sinh 2\alpha}{\cosh 2\alpha - \cos 2\beta}\right) \\
\sigma_z &= -\frac{2q}{\pi b} \frac{\lambda}{\lambda + \mu} e^{-\alpha} \sin\beta \\
\tau_{xy} &= -\frac{2q}{\pi b} \sinh\alpha \sin\beta \frac{\sin 2\beta}{\cosh 2\alpha - \cos 2\beta} \\
\tau_{yz} &= 0 \\
\tau_{xz} &= 0
\end{aligned}\right\} \quad (11)$$

where q is the loading per unit length of contact strip, λ and μ are Lame's constants and b is one-half the width of the contact strip. The equations of transformation are

$$\left.\begin{aligned}
y &= b \cosh\alpha \cos\beta \\
x &= b \sinh\alpha \sin\beta
\end{aligned}\right\} \quad (12)$$

where y and x are the rectangular coordinates. The locations of the points in elliptical coordinates used in Eqs. 11 are the intersection of the ellipse

$$\frac{y^2}{b^2 \cosh^2\alpha} + \frac{x^2}{b^2 \sinh^2\alpha} = 1 \quad (13)$$

with the hyperbola

$$\frac{y^2}{b^2 \cos^2\beta} - \frac{x^2}{b^2 \sin^2\beta} = 1 \quad (14)$$

* N. M. Belayev, loc. cit., page 12. Belayev's equations are also quoted in Stewart Way, Journ. of Applied Mechanics, ASME, 1935; and Fr. Karas, Forschung auf d. Gebiete d. Ingenieurwesens, VDI, Bd. 11, No. 6, 1940.

We can define the sin β and sinh α functions in terms of x and y by solving the Eqs. 13 and 14 as follows:

$$\left.\begin{aligned} \sin\beta &= \pm\sqrt{\frac{(b^2 - y^2 - x^2) + \sqrt{(b^2 - y^2 - x^2)^2 + 4b^2x^2}}{2b^2}} \\ \text{and} \\ \sinh\alpha &= \pm\sqrt{\frac{-(b^2 - y^2 - x^2) + \sqrt{(b^2 - y^2 - x^2)^2 + 4b^2x^2}}{2b^2}} \end{aligned}\right\} \quad (15)$$

The other functions in Eqs. 11 can be expressed in terms of α and β as

$$\begin{aligned} \cos\beta &= \sqrt{1 - \sin^2\beta} & \sinh 2\alpha &= 2\sinh\alpha\cosh\alpha \\ \cosh\alpha &= \sqrt{1 + \sinh^2\alpha} & \cosh 2\alpha &= \cosh^2\alpha + \sinh^2\alpha \\ \sin 2\beta &= 2\sin\beta\cos\beta & e^{-\alpha} &= \cosh\alpha - \sinh\alpha \\ \cos 2\beta &= 1 - 2\sin^2\beta \end{aligned} \quad (16)$$

By using Eqs. 15 and 11 the values of the stress components σ_x, σ_y, σ_z and τ_{xy} can be evaluated for any desired point having coordinates (x,y), and the normal and the shearing stress on any plane at these points of contact zone can now be found by selecting the proper angle φ and solving Eqs. 9 and 10. (See Fig. 6b)

11. Stress Variation in Contact Zone Caused by Rolling

Using Eqs. 11, 15, and 10 the values of the stress components and $\tau_{45°}$ were evaluated for a number of points located along lines parallel to the y-axis and at various distances from the contact surface. The calculations are summarized in Fig. 9 which shows the magnitude of the stress components, σ_x, σ_y, σ_z and τ_{xy}, in terms of p_{max}, the maximum pressure at the middle of the contact surface, plotted against the distance y from the plane of symmetry in terms of b. The four parts of Fig. 9 show these quantities for the four distances $x = 1.0\ b$, $0.78\ b$, $0.50\ b$ and $0.10\ b$ from the contact surface, respectively. Figures 9b and 9c also show curves of $\tau_{45°}$.

The curves in Fig. 9 also represent the influence lines of stresses at points in these layers. Thus, the curves not only give an idea about the maximum stresses at the desired point but also indicate the manner in which they vary during the loading cycle.

In Fig. 9a are plotted curves representing the stresses in the layer $x = 1.0\ b$ from the contact surface. Because the normal stresses σ_x and σ_z reach their maximum values in the plane of symmetry, they must occur when the point under consideration crosses the center line of cylinders. As this point moves away from the x-axis, these normal stresses gradually diminish and asymptotically approach zero. The curve of the normal stress σ_y has a saddle form symmetrical with the x-axis. The maximum

values of this stress are outside of the plane of symmetry. Therefore, the stress passes twice through its maximum value during the loading cycle. The shearing stress component τ_{xy} is equal to zero at the plane of symmetry, increasing at first and then approaching zero asymptotically as the contact point moves away from the x-axis. During the loading cycle these stresses change their absolute value as well as their direction. Thus, as the two cylinders are rolled together, the stress τ_{xy} changes from $-\tau_{xy}$ to $+\tau_{xy}$. This reversal of stress determines to a great extent the fatigue limit of the materials.

In Fig. 9b are shown the stresses σ_x, σ_y, σ_z, τ_{xy} and $\tau_{45°}$ in the layer $x = 0.78\ b$, where, according to Belayev and Thomas and Hoersch, the shearing stress reaches its maximum value.

The diagram shows that, even though the absolute value of the stress reaches its maximum in this layer, this stress apparently is not the determining factor in causing the material to fail under the existing conditions. It seems probable that the stress τ_{xy} has more to do with the fatigue failure. This stress has an absolute value somewhat smaller than the maximum value of $\tau_{45°}$, but changes its direction during the loading cycle. From this curve it is seen that the ordinates of the influence line τ_{xy} reach their maximum absolute values at points located between $y = \pm 0.75\ b$ and $y = \pm 1.0\ b$ from the line of symmetry.

In Fig. 9c are shown the influence lines of stress components and the shearing stress $\tau_{45°}$ in the layer which is a distance $x = 0.5\ b$ from the surface. Here the shearing stress τ_{xy} reaches about its maximum value. This maximum absolute value of these ordinates is located about $y = \pm 0.85\ b$ from the line of symmetry and has a magnitude of

$$(\tau_{xy})_{\max} \cong 0.256 p_{\max}$$

Finally Fig. 9d shows the stresses σ_x, σ_y, σ_z and τ_{xy} in a layer $x = 0.1\ b$ from the contact surface.

The results of the investigation of the stress condition on the surface ($x = 0$) are shown in Fig. 10. Here, the normal stresses σ_x and σ_y are equal to the pressure on the contact area, and their maximum value is equal to the maximum pressure on the middle of contact strip

$$(\sigma_x)_{\max} = (\sigma_y)_{\max} = 1.0 p_{\max} = \frac{2q}{\pi b}$$

Using the value for the Poisson's ratio as $\mu = 0.3$*, the maximum value of stress component σ_z at the surface is equal to

$$(\sigma_z)_{\max} = 0.6 p_{\max}$$

The shearing stress τ_{xy} on the surface is equal to zero.

* This value for the Poisson's ratio is also used in the other evaluations.

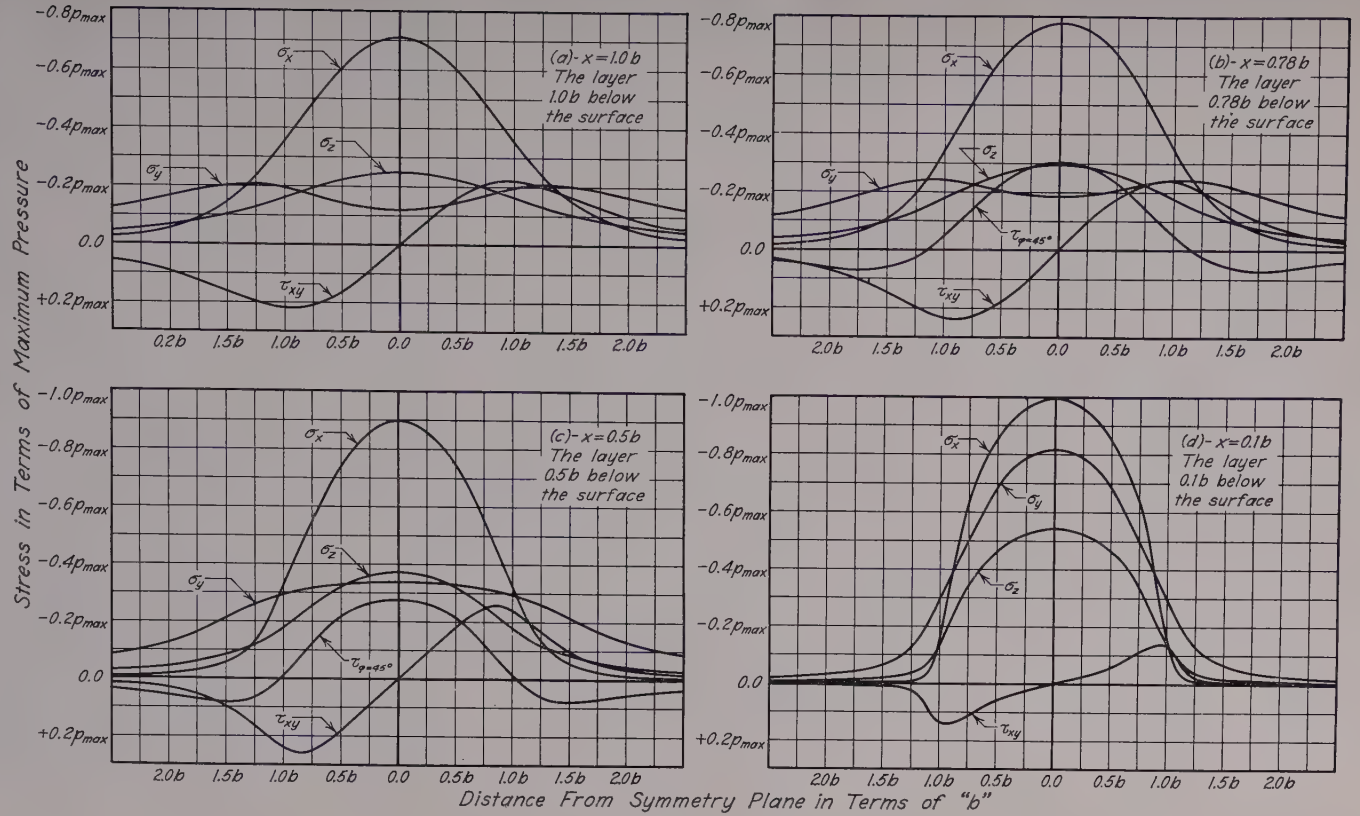

Fig. 9. Variation of Stress Components in Contact Zone During Loading Cycle

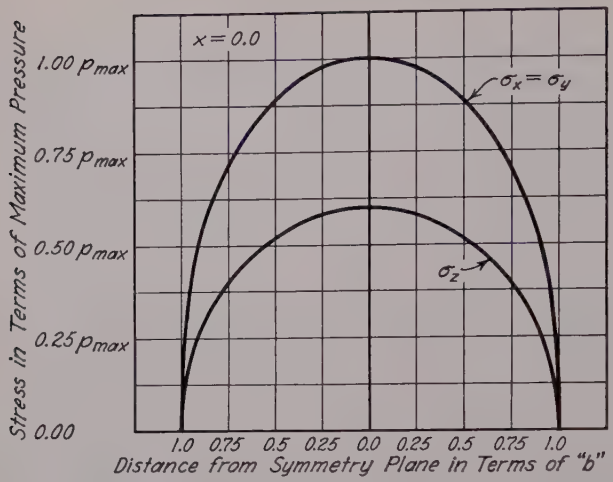

Fig. 10. Variation of Normal Stresses on Contact Surface During Loading Cycle

The data in Figs. 9 and 10 are incorporated with those given in Table 1. The values tabulated for σ_x, σ_y, σ_z and $\tau_{45°}$ refer to these stresses which occur at the axis of symmetry in the x–z plane. These are maximum values except for σ_y in layers farther away than $x = 0.5\ b$. Also listed are the maximum values of the shearing stress τ_{xy}, which occur outside the axis of symmetry. The range ratios of $\tau_{45°}$ during a stress cycle are listed in the last column in Table 1. These range ratios are the ratio of algebraical values of minimum stress to maximum stress during the cycle. That is

$$r = \frac{\sigma_{\min}}{\sigma_{\max}}; \qquad r = \frac{\tau_{\min}}{\tau_{\max}}$$

The normal stresses σ_x, σ_y and σ_z all vary from zero to negative maximum; therefore $\sigma_{\min} = 0$ and the value of the range ratio is always

$$r = \frac{0}{\sigma_{\max}} = 0$$

The shearing stress τ_{xy}, on the other hand, varies from a positive maximum to a negative maximum value; hence the range ratio is always

$$r = \frac{-\tau_{\max}}{+\tau_{\max}} = -1 \ ,$$

The stress $\tau_{45°}$ changes in an asymmetrical cycle which gives rise to a range ratio whose value depends on the distance x from the contact surface. At the point where it reaches its maximum value the range ratio for $\tau_{45°}$ is approximately

$$r \cong -0.25$$

Several authors, including Belayev, Thomas and Hoersch, Schmitter, Petrusievich and others, believe that the critical point of the contact zone should be taken as the point where the maximum shearing

Table 1

Maximum Values of Stress in Contact Zone in Terms of p_{max}

Distance from Contact Surface, x	Maximum Stresses* in Terms of					Range Ratio of Stress $\tau_{45°}$
	σ_y	σ_x	σ_z	τ_{xy}	$\tau_{45°}$	
0.0	−1.000	−1.000	−0.600	±0.000	0.000	.....
0.1 b	−0.815	−0.995	−0.543	±0.146	0.090	.....
0.2 b	−0.659	−0.980	−0.492	±0.195	0.160	.....
0.5 b	−0.342	−0.894	−0.371	±0.256	0.276	−0.29
0.78 b	−0.188	−0.788	−0.293	±0.233	0.300	−0.25
1.0 b	−0.121	−0.707	−0.248	±0.218	0.293	−0.21
1.2 b	−0.084	−0.640	−0.217	±0.205	0.267	.....
1.5 b	−0.054	−0.552	−0.182	±0.178	0.248	.....

* The values tabulated for σ_x, σ_y, σ_z and $\tau_{45°}$ refer to the stresses which occur at the axis of symmetry in the x–z plane. The stresses τ_{xy} occur outside of the plane of symmetry, while the stresses σ_y given for x greater than about 0.5 b are those on the axis of symmetry and are somewhat less than $(\sigma_y)_{max}$.

stress occurs. If this is true, then the critical point lies in the layer at a distance $x = 0.78\ b$ from the contact surface where maximum shearing stress reaches its highest value

$$(\tau_{45°})_{max} \cong 0.3 p_{max}$$

However, this way of determining the critical point would seem to be restricted to the conditions of constant loading and would not be valid for variable stress conditions existing when two compressed cylinders are rolling. If we consider the shearing stress critical, for the case of rolling cylinders, it would seem more reasonable to take the critical point nearer to the surface where the maximum stress τ_{xy} occurs. Although the absolute value of $(\tau_{xy})_{max}$ is lower, its range ratio is always equal to minus one, constituting a complete stress reversal.

V. STRENGTH CONDITIONS OF MATERIALS SUBJECTED TO VARIABLE CONTACT STRESSES

It has already been mentioned that some authors have based their strength calculations on the maximum pressure at the contact surface. Others base the strength on the maximum shearing stresses. There is no real difference between the two methods since the maximum shearing stresses are directly proportional to the maximum pressure on the contact surface. However, neither one of these methods for determining the critical and permissible loads takes into consideration the complex stress conditions due to the variable contact loading.

By knowing the absolute values and range ratios of stresses at various layers in the contact zone, it is now possible to develop an equation for expressing the conditions of strength based on these variable stresses. Normal and shearing stress data, the manner in which they change, and the properties of materials important in fatigue strength determinations are used in arriving at this relationship.

12. Huber-Mises' Condition on Static Loading

According to the opinion of some investigators, there is good correlation between theoretical calculations based on the Huber-Mises' hypothesis and experimental results for the case of plane stress conditions. By this hypothesis, the strength condition for constant loading can be expressed by the equation:

$$\sigma_1^2 + \sigma_2^2 - \sigma_1\sigma_2 = \sigma_s^2 \tag{17}$$

where σ_1 and σ_2 are the principal stresses and σ_s is the yield point of the material. The same condition expressed in terms of the components (see Appendix A) can be written in the form:

$$(\sigma_x + \sigma_y)^2 - 3\sigma_x\sigma_y + 3\tau_{xy}^2 = \sigma_s^2 \tag{18}$$

In order to satisfy the correlation existing between the torsional yield point and the tensile or compressive yield point for different materials, a correction factor should be introduced in the plastic condition (see Sorensen* and Lahmann†). With this correction, Eq. 17 takes the form:

$$(\sigma_1 + \sigma_2)^2 - \left(\frac{\sigma_s}{\tau_s}\right)^2 \sigma_1\sigma_2 = \sigma_s^2 \tag{19}$$

* S. V. Sorensen, "Theory of Strength in Variable Loading," Inst. of Appl. Mech. N. 33, Academy of Sciences of the Ukrainian SSR, Kiev, 1938. (Ukrainian)
† K. Lahmann, Ingenieur, Archiv. H. 3, 1930

or using the components σ_x, σ_y and τ_{xy} (see Appendix B)

$$(\sigma_x + \sigma_y)^2 - \left(\frac{\sigma_s}{\tau_s}\right)^2 (\sigma_x\sigma_y - \tau_{xy}^2) = \sigma_s^2 \tag{20}$$

13. General Case of Plane Stress Condition Due to Variable Loading

Equation 18 can be applied to the general case of plane stress condition due to variable loading as was shown by Sorensen. In this case, Eq. 18 becomes

$$\left[\left(\frac{\sigma_{xm}}{\sigma_s} + \frac{\sigma_{xv}}{\sigma_{-1}}\right) + \left(\frac{\sigma_{ym}}{\sigma_s} + \frac{\sigma_{yv}}{\sigma_{-1}}\right)\right]^2 - 3\left[\left(\frac{\sigma_{xm}}{\sigma_s} + \frac{\sigma_{xv}}{\sigma_{-1}}\right)\left(\frac{\sigma_{ym}}{\sigma_s} + \frac{\sigma_{yv}}{\sigma_{-1}}\right)\right] + 3\left[\frac{\tau_m}{\sigma_s} + \frac{\tau_v}{\sigma_{-1}}\right]^2 = 1 \tag{21}$$

In this equation the stresses are reduced to a statical form according to Goodman's linear relation as shown in Appendix C. The reduced stresses are

$$(\sigma_x)_r = \sigma_{xm} + \frac{\sigma_s}{\sigma_{-1}}\sigma_{xv}; \quad (\sigma_y)_r = \sigma_{ym} + \frac{\sigma_s}{\sigma_{-1}}\sigma_{yv}; \quad \tau_r = \tau_m + \frac{\tau_s}{\tau_{-1}}\tau_v$$

where

σ_{xv}, σ_{yv} and τ_v are the amplitudes of the alternating parts of the stress components

σ_{xm}, σ_{ym} and τ_m are the steady parts

σ_s and τ_s the yield point and

σ_{-1} and τ_{-1} the endurance limits due to a symmetrical stress cycle ($r = -1$)

By using the reduced stresses, Eq. 20 can be written:

$$\left[\left(\frac{\sigma_{xv}}{\sigma_{-1}} + \frac{\sigma_{xm}}{\sigma_s}\right) + \left(\frac{\sigma_{yv}}{\sigma_{-1}} + \frac{\sigma_{ym}}{\sigma_s}\right)\right]^2 - \left(\frac{\sigma_s}{\tau_s}\right)^2\left[\left(\frac{\sigma_{xv}}{\sigma_{-1}} + \frac{\sigma_{xm}}{\sigma_s}\right)\left(\frac{\sigma_{yv}}{\sigma_{-1}} + \frac{\sigma_{ym}}{\sigma_s}\right)\right] + \left[\frac{\tau_v}{\tau_{-1}} + \frac{\tau_m}{\tau_s}\right]^2 = 1 \tag{22}$$

For the case of variable stress conditions the extreme value of normal stress components must be put into this equation. Therefore, the normal stress σ_x and σ_z must be put into Eq. 22 to determine the strength of the material in the layer very near the surface. To determine the strength of layer of material further from the surface, where $x \geqq 0.5\ b$, the normal stress components σ_x and σ_y must be used (see Table 1 and Figs. 9–10).

14. Endurance Limit of Steels Subjected to Variable Compressive Stress

There are sufficient data about the endurance limits of steels due to symmetrical alternate loading but not about the endurance limit

for the case of the asymmetrical loading cycle. The endurance limit of steels due to variable compressive stress with a zero range ratio is considerably higher than the same limit for tensile stresses. According to R. Thomas' and I. Lowther's data*, steel having a tensile yield point about 37,000 lb per sq in. and tensile strength about 60,000 lb per sq in. has a compressive endurance limit $\sigma_{op} = 48{,}000$ lb per sq in. These results are somewhat conditional because the specimens which had an asymmetrical cross section were tested by repeated bending and the maximum compressive stresses were determined by the expression $\sigma_{op} = M/Z$ where M is the bending moment and Z is the section modulus.

This method would be correct to use if the stresses at the points under consideration were not higher than the yield point. Since this is not the case, it is reasonable to expect a plastic deformation at the points of maximum stresses, and consequently a change in the distribution of the stresses at the cross section of the specimen. Because of this phenomenon, the maximum value of the actual stress in the zone of compression will be smaller than the value calculated from the expression above. Nevertheless, these experiments show that the value of σ_{op} is close to the yield point.

G. Seeger†, H. F. Moore‡, J. O. Smith¶ and some other investigators also considered the problem of fatigue failure under repeated compression. Investigations on the fatigue strength of a carbon steel and a high-strength heated alloy steel by asymmetrical loading cycles were also made by the author§ and were found to have the following properties:

	Carbon Steel	Ni-Cr-Mo Steel
Ultimate tensile strength, σ_u	78 700 psi	257 500 psi
Yield point, $\sigma_{s_{0.2}}$	45 500 psi	172 000 psi
Elastic limit, $\sigma_{0.003}$		152 000 psi
Brinell hardness number, H_B	155–157	477
Percent elongation, δ_{10}	25.5	5.5
Percentage area reduction, ψ	53.7	14.0
Fatigue strength for symmetrical tensile-compressive cycle, σ_{-1}	25 000 psi	64 000 psi
Fatigue strength for tensile loading from zero to maximum, σ_{ot}	37 700 psi	89 600 psi
Fatigue strength for compressive loading from zero to maximum, σ_{op}	49 200 psi	160 800 psi
Fatigue strength for compression with cycle ratio, $r = +0.2$; $\sigma_{0.2p}$	54 000 psi	

* R. Thomas and I. Lowther, ASTM Proceedings of the Thirty-fifth Annual Meeting, Vol. 32, Part II, June 1932.

† G. Seeger, Wirkung von Drückvorspannung auf die Dauerfestigkeit metallischer Werkstoffe, VDI, Berlin, 1935.

‡ H. F. Moore, Report of the Rails Investigation for the Quarter Ending December 31, 1932. Univ. of Ill. Eng. Exp. Sta.

¶ J. O. Smith, "The Effect of Range of Stress on the Fatigue Strength of Metals," Univ. of Ill. Eng. Exp. Sta. Bul. No. 334, 1942.

§ E. I. Radzimovsky, Report of Institute of Appl. Mech. of Academy of Sciences of Ukrainian SSR, 1940 (Unpublished).

The results of these experiments are shown on the Goodman diagrams in Fig. 11. The steady parts of the stresses are scaled along the abscissa and the limiting stresses along the ordinate.

The above mentioned experiments, and others in the same field, indicate that the fatigue limit of steel due to variable compressive stresses with a zero range ratio is near to the tensile yield point, or somewhat higher. Thus, it is possible to use

$$\sigma_{op} = \sigma_s \tag{23}$$

for calculation purposes.

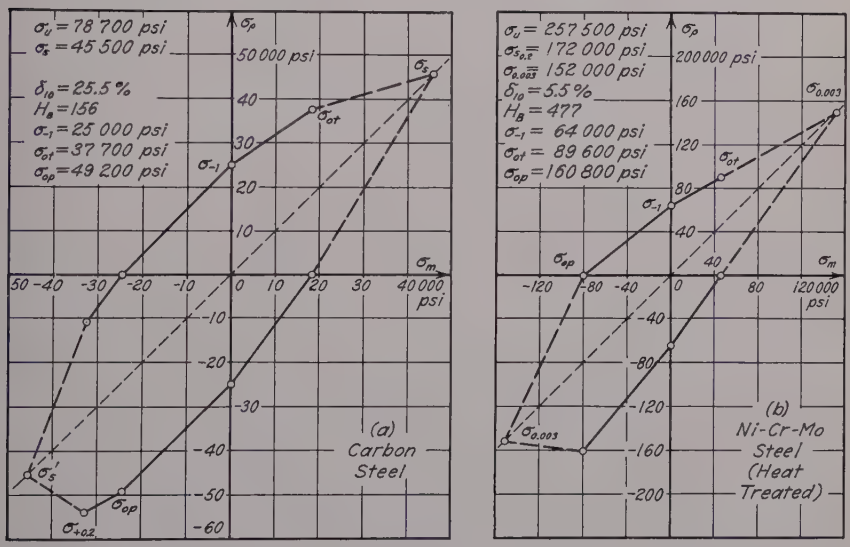

Fig. 11. Strength Limits of Steels Subjected to Asymmetrical Loading Cycles

15. Strength Condition of Materials Subjected to Contact Stresses Produced by Two Cylinders Rolling

As shown in Section 11, the range ratio of the normal stresses σ_x, σ_y and σ_z is $r = 0$, and the range ratio of the stress τ_{xy} is $r = -1$ for the case of two rolling cylinders pressed together. Therefore,

$$\frac{\sigma_{xm}}{\sigma_s} + \frac{\sigma_{xv}}{\sigma_{-1}} = \frac{\sigma_{xm} + \sigma_{xv}}{\sigma_{op}}; \quad \frac{\sigma_{ym}}{\sigma_s} + \frac{\sigma_{yv}}{\sigma_{-1}} = \frac{\sigma_{ym} + \sigma_{yv}}{\sigma_{op}}$$

$$\frac{\sigma_{zm}}{\sigma_s} + \frac{\sigma_{zv}}{\sigma_{-1}} = \frac{\sigma_{zm} + \sigma_{zv}}{\sigma_{op}}; \quad \tau_m = 0; \quad \tau_v = \tau_{xy} \tag{24}$$

In addition

$$\sigma_{xm} + \sigma_{xv} = \sigma_x; \quad \sigma_{ym} + \sigma_{yv} = \sigma_y; \quad \sigma_{zm} + \sigma_{zv} = \sigma_z; \quad \sigma_{op} = \sigma_s \tag{24a}$$

where σ_{op} is the endurance limit on pressure by the range ratio $r = 0$, and σ_s is the tensile yield point. By substituting Eqs. 24 and 24a into Eq. 22, it is simplified considerably to

$$\left(\frac{\sigma_x + \sigma_y}{\sigma_s}\right)^2 - \left(\frac{\sigma_s}{\tau_s}\right)^2 \left(\frac{\sigma_x \sigma_y}{\sigma_s^2}\right) + \left(\frac{\tau_{xy}}{\tau_{-1}}\right)^2 = 1 \tag{25}$$

Equation 25 shows the strength condition of steel in the contact zone of two rolling cylinders. From Table 1, it is evident that values for σ_x and σ_y must be used in the strength calculations for points which are in layers a distance $x \geqq 0.5\ b$ from the surface. For points nearer the surface than $0.5\ b$, σ_x and σ_z, which are now the extreme stresses, must be used in the calculations. In this case, Eq. 25 must be modified to

$$\left(\frac{\sigma_x + \sigma_z}{\sigma_s}\right)^2 - \left(\frac{\sigma_s}{\tau_s}\right)^2 \left(\frac{\sigma_x \sigma_z}{\sigma_s^2}\right) + \left(\frac{\tau_{xy}}{\tau_{-1}}\right)^2 = 1 \tag{25a}$$

As was shown previously, the various stress components are not in phase. The maximum of the stresses σ_x and σ_z both occur at the plane of symmetry, at which points the stress τ_{xy} is equal to zero. The stress τ_{xy}, on the other hand, reaches its maximum value outside of the plane of symmetry. It would seem that this circumstance could influence the conditions for failure. However, the results of experiments conducted by Sorensen* show that such is not the case. Sorensen tested a steel specimen by a simultaneous repeated loading in bending and torsion. Two series of experiments were conducted. In the first the cycles for bending and torsion loading were in phase. In the second series of tests the cycles were out of phase by 90 deg. The fatigue curves plotted from the data of these tests were the same for both loading conditions. It was concluded that the endurance limit is not affected by the difference in phase relationships of the stress components.

The values of σ_x, σ_y, σ_z and τ_{xy} can be evaluated in terms of $p_{\max}$, which is the maximum pressure on the contact strip, for any point in the contact zone. The value $p_{\max}$ depends upon the magnitude of loading and upon the size, form, and mechanical properties of the materials of the two compressed bodies. It can be calculated using Eqs. 2 and 5.

The limiting value of the maximum pressure at which the initial fatigue failure in the contact zone is expected is the critical value of $p_{\max}$

* S. Sorensen, "About the Strength Conditions in Variable Loadings for the Plane and Volume Stress Condition," Eng. Mag. Inst. Mechan. Acad. of Sciences of USSR, Vol. I, ser. 1, 1941. (Russian)

and is denoted by the symbol σ_g. Since the stresses σ_x, σ_y, σ_z and τ_{xy} at any point in the contact zone are directly dependent upon the value of p_{max}, they can also be expressed in terms of σ_g, as follows:

$$\sigma_x = \alpha\sigma_g; \quad \sigma_y = \beta\sigma_g; \quad \sigma_z = \gamma\sigma_g; \quad \tau_{xy} = \delta\sigma_g \tag{26}$$

Using these relationships, Eq. 25 now can be expressed as

$$\frac{\sigma_g^2}{\sigma_s^2}(\alpha+\beta)^2 - \left(\frac{\sigma_s}{\tau_s}\right)^2 \alpha\beta \frac{\sigma_g^2}{\sigma_s^2} + \delta^2 \frac{\sigma_g^2}{\tau_{-1}^2} = 1$$

from which

$$\sigma_g = \sqrt{\frac{\sigma_s^2}{(\alpha+\beta)^2 - \alpha\beta\left(\frac{\sigma_s}{\tau_s}\right)^2 + \delta^2\left(\frac{\sigma_s}{\tau_{-1}}\right)^2}} \tag{27}$$

Letting $A=(\alpha+\beta)^2$, $B=\alpha\beta$ and $C=\delta^2$, Eq. 27 can be written

$$\sigma_g = \frac{\sigma_s}{\sqrt{A - B\left(\frac{\sigma_s}{\tau_s}\right)^2 + C\left(\frac{\sigma_s}{\tau_{-1}}\right)^2}} \tag{28}$$

or more compactly as

$$\sigma_g = K\sigma_s \tag{29}$$

where

$$K = \frac{1}{\sqrt{A - B\left(\frac{\sigma_s}{\tau_s}\right)^2 + C\left(\frac{\sigma_s}{\tau_{-1}}\right)^2}} \tag{30}$$

The coefficient K in Eqs. 29 and 30 shows the relationship between the yield point, σ_s, of the material and the critical pressure, σ_g, on the surface. The values α, β, and δ, and thus A, B, and C, depend only on the position of the point under consideration, while K and hence σ_g, the critical pressure on the contact surface, depend upon properties of the materials making up the bodies as well as the distance of the layer from the surface.

The critical layer in the contact zone is that one for which the value of σ_g is a minimum. This minimum value of σ_g is called the "surface endurance limit" of two rolling cylinders.

Since the extreme values of normal stress components are required in Eqs. 27-30, the coefficient A is equal to $(\alpha+\beta)^2$ and coefficient B to $\alpha\beta$ for points at a distance of $x \geqq 0.5\ b$; the coefficient A is equal to $(\alpha+\gamma)^2$ and coefficient B to $\alpha\gamma$ for points at a distance of $x < 0.5\ b$.

VI. RESULTS OF INVESTIGATIONS USING THE SUGGESTED STRENGTH CONDITION

Knowing the mechanical properties of the materials, it is possible now to find the critical value σ_g. The steels considered were the soft carbon steels up to the high-strength alloy steels. The mechanical properties of the steels used for the calculations are given in Table 2.

Table 2

Mechanical Properties of Steels

Sample No.	Type of Steel	Mechanical Properties, psi			
		Tensile Yield Point σ_s	Tensile Strength σ_u	Torsional Yield Point τ_s	Endurance Limit in Torsion τ_{-1}
1	Carbon	35 600	64 200	24 200	15 700
2	Carbon	44 200	78 300	27 000	19 900
3	Carbon	59 800	98 300	37 000	27 000
4	Chrome-Nickel	88 300	118 000	54 100	34 000
5	Chrome-Nickel-Vanadium	135 000	156 000	85 300	42 200
6	Chrome-Nickel-Molybdenum	142 200	170 500	86 800	42 700

In Table 3 are tabulated the values of coefficients A, B, and C for points located at various distances from the surface. The coefficients K for the various steels presented in Table 2 are also listed. The data in bold face type in Table 3 are for the points below the surface where σ_g has the smallest value. It is reasonable to expect that the fatigue crack starts in a corresponding layer in the contact zone.

The distance of the critical layer from the surface depends upon the mechanical properties of the steels. Table 3 shows that the critical layer for soft steels is closer to the surface than for the hard steels, but for all steels, these critical layers are closer to the surface than the point of maximum shearing stress.

Table 3

Coefficients A, B, and C and the Ratio, K, Between Critical Pressure on the Surface and Yield Point of Different Steels, for Various Layers Below Contact Surface

Distance from Surface, x	Coefficients			Ratio $K=\sigma_g/\sigma_s$ for Steel No.					
	A	B	C	1	2	3	4	5	6
0.0	2.560	0.600	0.0000	0.889	1.025	1.003	1.018	0.972	1.026
0.1 b	2.365	0.540	0.0213	**0.873**	0.989	0.971	0.965	0.901	0.931
0.2 b	2.161	0.482	0.0380	**0.872**	**0.972**	**0.961**	**0.938**	0.862	0.881
0.5 b	1.528	0.306	0.0655	0.909	0.985	0.976	**0.930**	**0.827**	**0.8205**
0.78 b	0.953	0.1482	0.0543	1.046	1.102	1.095	1.039	0.935	0.929
1.0 b	0.6856	0.0855	0.0475	1.157	1.125	1.199	1.134	1.020	1.008
1.2 b	0.5242	0.0538	0.042	1.275	1.304	1.302	1.227	1.102	1.087
1.5 b	0.367	0.0298	0.0317	1.465	1.502	1.499	1.413	1.388	1.251

These results possibly explain some of the discrepancies among the data of previous investigators who used the roller testing machines in order to study the character of failure and fatigue limit due to the repeated contact stresses arising from two rolling cylinders. In connection with this, the observation of M. Turkish* about failure on the faces of tappets of valve gears should be mentioned. This author stated that the failure in overstressed steel tappet faces originated in the form of microscopic cracks on the surface, but in the case of a chilled cast-iron tappet, a fatigue crack starts beneath the surface.

The values obtained by using Eq. 28 are shown in the diagram of Fig. 12. The abscissa represents the yield points of steels and the ordinate represents the surface endurance limit.

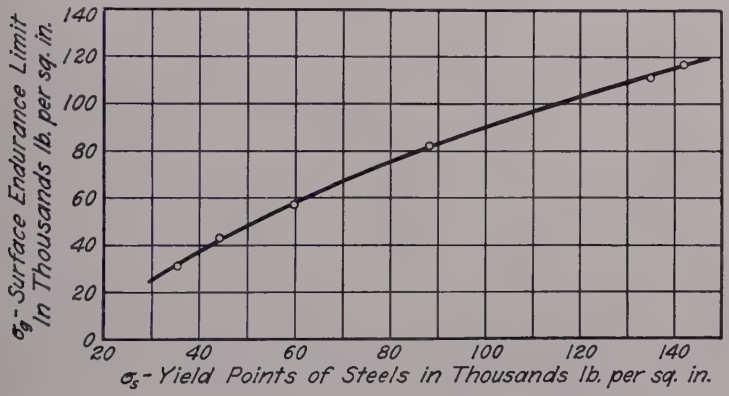

Fig. 12. Surface Endurance Limit of Two Rolling Cylinders

The diagram of Fig. 13 shows the comparison between the data found using Eq. 28, the results of S. Way's experiments on rollers, and surface endurance limits which are recommended by E. Buckingham for the gear drives. This comparison shows that there is quite satisfactory correlation between data obtained by calculation and the experimental results. Buckingham's tables gave relationships between surface endurance limit and the hardness of materials. Because of this, the abscissas in Fig. 13 represent the Brinell hardness. Dëhmer's† relation

$$H_B = \frac{\sigma_u - 4.8}{0.343}$$

where H_B = Brinell hardness number and σ_u = tensile strength of steel in kg per sq mm, was used for reducing the strength of materials to their hardness number.

* M. C. Turkish, loc. cit., page 8.
† P. Dëhmer, Die Brinellsche Kugeldruckprobe, Berlin, 1935.

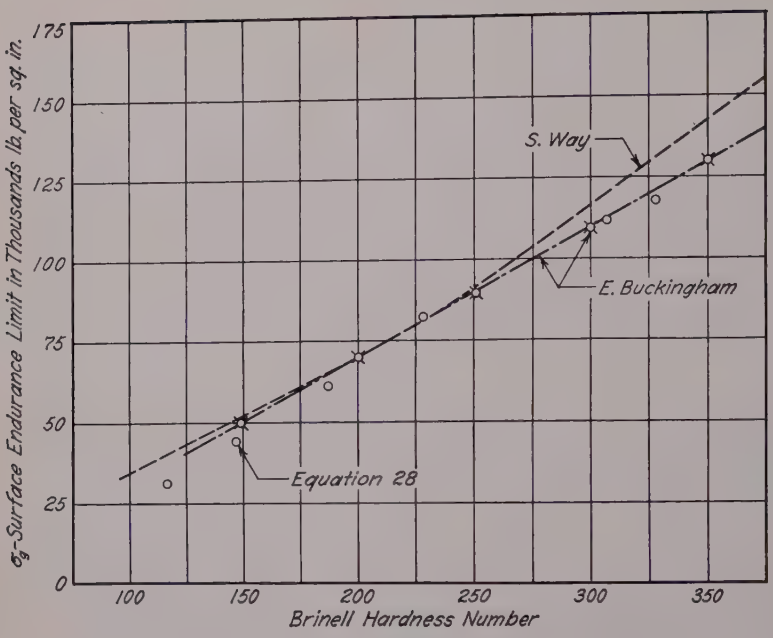

Fig. 13. Comparison Between Data from Eq. 28 and Experimental Results

The method presented in this bulletin for strength calculations does not consider the number of factors which could influence the strength. For example, the presence of a lubricating layer between the two bodies in contact affects, to some degree, the load distribution at the contact surface. The stress gradient in the contact zone which affects the strength of material and the effect of the cold working are also not considered. However, since the other methods currently in use do not consider these factors either, no great importance is attached to their omission. On the other hand the method suggested here does seem to consider more completely the stresses occurring in the contact zone and the manner in which these stresses vary, as well as the properties of the materials upon which the strength of machine members in the contact zone depends.

VII. SUMMARY AND CONCLUSIONS

The strength determination in the contact zone of two compressed cylinders rolling together should take into account the manner in which the stresses vary during a loading cycle, as well as the properties of the materials upon which the strength depends.

Two methods are suggested for determining the manner in which the stresses vary during the loading cycle.

a) The first method consists of substituting a system of concentrated forces for the given load distribution across the contact strip and using the influence lines due to these forces.

b) The second method consists of using Belayev's equations expressed in elliptic coordinates and transforming coordinates; introducing into these equations the locations of the points under consideration determined in Cartesian coordinates; and then determining the values of the stress components at any point in the contact zone, including points outside the plane of symmetry.

The manner in which the stress components change during the loading cycle at the various layers in the contact zone were investigated. The principal results were:

a) The normal stresses σ_x and σ_z change during the loading cycle as follows: $0 \rightarrow \sigma_{max} \rightarrow 0$, with the maximum absolute value occurring at the plane of symmetry. These stresses approach zero asymptotically.

b) The curves of the normal stress component σ_y has a saddle form symmetrical about the x-axis at distances approximately greater than $0.5\ b$ from the contact surface. In this case, the maximum values of the stress are outside of the plane of symmetry. Therefore, the stress component in these layers passes twice through its maximum value during the loading cycle.

c) The stress $\tau_{45°}$ reaches maximum values in the plane of symmetry at a distance about $x = 0.78\ b$ from the contact surface. This stress has various range ratios, which depend upon the distance of the points from the surface. At the points where $x = 0.78\ b$, the stress $\tau_{45°}$ changes with the range ratio $r \cong -0.25$; the maximum range ratio is about $r = -0.29$ at the layer where $x \cong 0.5\ b$.

d) Based on the strength of materials subjected to repeated loading, the shearing stress τ_{xy} is the critical stress. This stress is equal to zero at the plane of symmetry and changes in a symmetrical cycle with a

range ratio $r = -1$. The maximum value of $\tau_{xy} \cong -0.256 p_{max}$ occurs in the layer where $x \cong 0.5\ b$. The maximum τ_{xy} does not coincide in phase with the maximum normal stresses and maximum shearing stress.

Calculations based only on maximum normal stresses or on the maximum shearing stress cannot be considered as satisfactory, because of the complicated stress conditions which are present in the case of two compressed cylinders rolling together. The expression for the strength condition based on the Huber-Mises' hypothesis is suggested. The data on stress variations during the loading cycles, as well as the fatigue properties of materials, are used.

A table was made showing the values of critical pressure on the surface in terms of the yield point of different steels for various layers below the contact surfaces of two rolling cylinders. The data in this table which are based on the calculations of dynamic strength of materials differ from the results of calculation in which the contact stress condition was considered as a statical problem. The table shows that the relation between the yield point of steels and the critical pressure on the contact surface is not constant but depends upon the mechanical properties of materials. It shows that the distance of the critical layer from the contact surface also depends upon the mechanical properties of the steels. For the soft steels this layer is closer to the surface than for the hard steels. For all steels this layer is closer to the surface than the point of maximum shearing stress.

Diagrams were made showing the relations between the critical pressure on the surface and the yield points and hardness of the materials. The last diagram shows good correlation with experimental data.

Further experimental verification of the results is desirable. It would be particularly desirable to find experimentally the actual location where the initial fatigue crack begins in the contact zone. Results from such an investigation would help to evaluate the validity of the existing theories of failure for the strength conditions under consideration.

APPENDIX A. TRANSFORMATION OF EQ. 17 IN TERMS OF THE STRESS COMPONENTS

According to the Huber-Mises' hypothesis, the conditions of plastic deformation by statical loading are expressed by Eq. 17 in the text:

$$\sigma_1^2 + \sigma_2^2 - \sigma_1\sigma_2 = \sigma_s^2 \tag{17}$$

where σ_1 and σ_2 are the principal stresses

σ_s is the yield point of the material

For expressing this condition in terms of the stress components we can use the known relationships:

$$\sigma_1 = \frac{1}{2}(\sigma_y + \sigma_x) + \frac{1}{2}\sqrt{(\sigma_y - \sigma_x)^2 + 4\tau_{xy}^2} \tag{31}$$

and

$$\sigma_2 = \frac{1}{2}(\sigma_y + \sigma_x) - \frac{1}{2}\sqrt{(\sigma_y - \sigma_x)^2 + 4\tau_{xy}^2} \tag{32}$$

By substituting Eqs. 31 and 32 into Eq. 17, it takes the form:

$$\begin{aligned}\sigma_1^2 + \sigma_2^2 - \sigma_1\sigma_2 = &\left[\frac{1}{2}(\sigma_y + \sigma_x) + \frac{1}{2}\sqrt{(\sigma_y - \sigma_x)^2 + 4\tau_{xy}^2}\right]^2 \\ &+ \left[\frac{1}{2}(\sigma_y + \sigma_x) - \frac{1}{2}\sqrt{(\sigma_y - \sigma_x)^2 + 4\tau_{xy}^2}\right]^2 \\ &- \left[\frac{1}{2}(\sigma_y + \sigma_x) + \frac{1}{2}\sqrt{(\sigma_y - \sigma_x)^2 + 4\tau_{xy}^2}\right] \\ &\times \left[\frac{1}{2}(\sigma_y + \sigma_x) - \frac{1}{2}\sqrt{(\sigma_y - \sigma_x)^2 + 4\tau_{xy}^2}\right] = \sigma_s\end{aligned} \tag{33}$$

Letting

$$\frac{1}{2}(\sigma_y + \sigma_x) = a \tag{34}$$

and

$$\frac{1}{2}\sqrt{(\sigma_y - \sigma_x)^2 + 4\tau_{xy}^2} = b \tag{35}$$

then by substitution

$$\sigma_1^2 + \sigma_2^2 - \sigma_1\sigma_2 = (a + b)^2 + (a - b)^2 - (a + b)(a - b) = a^2 + 3b^2 = \sigma_s^2$$

or

$$\left[\frac{1}{2}(\sigma_y + \sigma_x)\right]^2 + 3\left[\frac{1}{2}\sqrt{(\sigma_y - \sigma_x)^2 + 4\tau_{xy}^2}\right]^2 = \sigma_s^2$$

Simplifying and collecting terms

$$\sigma_y^2 + \sigma_x^2 - \sigma_x\sigma_y + 3\tau_{xy}^2 = \sigma_s^2$$

or

$$(\sigma_x + \sigma_y)^2 - 3\sigma_x\sigma_y + 3\tau_{xy}^2 = \sigma_s^2 \qquad (18)$$

APPENDIX B. TRANSFORMATION OF EQ. 19 IN TERMS OF THE STRESS COMPONENTS

Equation 19 can be transformed by the same procedure used in Appendix A. It has the form

$$(\sigma_1 + \sigma_2)^2 - \left(\frac{\sigma_s}{\tau_s}\right)^2 \sigma_1\sigma_2 = \sigma_s^2 \tag{19}$$

Using Eqs. 31 and 32, 19 can be written

$$\begin{aligned}\sigma_s^2 = &\left[\frac{1}{2}(\sigma_y + \sigma_x) + \frac{1}{2}\sqrt{(\sigma_y - \sigma_x)^2 + 4\tau_{xy}^2}\right. \\ &\left. + \frac{1}{2}(\sigma_y + \sigma_x) - \frac{1}{2}\sqrt{(\sigma_y - \sigma_x)^2 + 4\tau_{xy}^2}\right]^2 \\ &- \left(\frac{\sigma_s}{\tau_s}\right)^2 \left[\frac{1}{2}(\sigma_y + \sigma_x) + \frac{1}{2}\sqrt{(\sigma_y - \sigma_x)^2 + 4\tau_{xy}^2}\right] \\ &\times \left[\frac{1}{2}(\sigma_y + \sigma_x) - \frac{1}{2}\sqrt{(\sigma_y - \sigma_x)^2 + 4\tau_{xy}^2}\right]\end{aligned} \tag{36}$$

By putting Eqs. 34 and 35 into Eq. 36,

$$\sigma_s^2 = [a+b+a-b]^2 - \left(\frac{\sigma_s}{\tau_s}\right)^2 (a+b)(a-b) = (2a)^2 - \left(\frac{\sigma_s}{\tau_s}\right)^2 (a^2 - b^2)$$

then by substituting 34 and 35 for a and b again and simplifying,

$$(\sigma_x + \sigma_y)^2 - \left(\frac{\sigma_s}{\tau_s}\right)^2 (\sigma_x\sigma_y - \tau_{xy}^2) = \sigma_s^2 \tag{20}$$

APPENDIX C. REDUCTION OF VARIABLE STRESSES TO STATICAL CONDITIONS

In Eqs. 21 and 22 the stresses are reduced to a statical form according to Goodman's linear relation. The Goodman's linear strength relationship is represented in Fig. 14.

If the stress varies in an asymmetrical cycle with some range ratio r, its maximum value, σ_r, consists of a steady part, σ_m, and an alternating part σ_v. For reducing this variable stress, σ_r, to a statical form, we have to take its steady part, σ_m, and add it to the alternating part σ_v, reduced to the statical condition. For statical loading the strength of the material will be greater than that for the alternate loading by a factor σ_s/σ_{-1}, where σ_s is the yield point and σ_{-1} the endurance limit due to a symmetrical stress cycle. Thus to reduce the part σ_v to the statical condition, we have to multiply the alternating part σ_v by σ_s/σ_{-1}. The reduced stress σ_r therefore takes the form:

$$\sigma_r = \sigma_m + (\sigma_v)_{\text{red}} = \sigma_m + \frac{\sigma_s}{\sigma_{-1}}\sigma_v$$

and

$$\tau_r = \tau_m + \frac{\tau_s}{\tau_{-1}}\tau_v$$

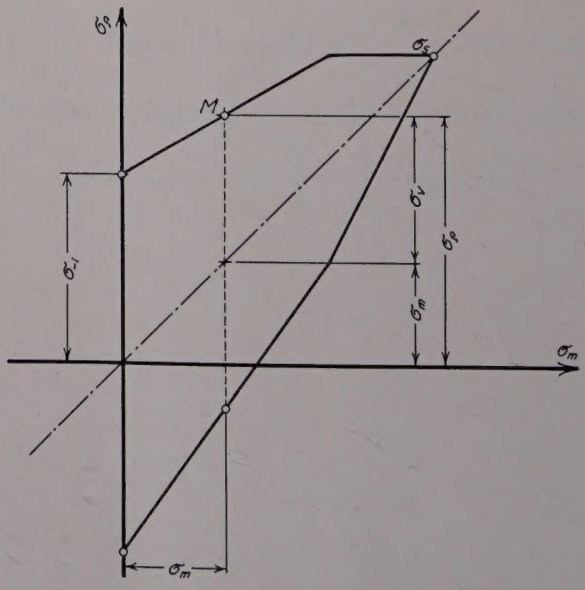

Fig. 14. Goodman's Linear Strength Relationship